Optimization of grillage design for the transportation of suction caisson jackets

Maria Athanasia Tsota

Delft University of Technology

TU Delft

Optimization of grillage design for the transportation of suction caisson jackets

by

Maria Athanasia Tsota

Student Name	Student Number
Maria Athanasia Tsota	5353130

Company:	Offshore Independents
Supervisor from TUDelft:	P.van der Male
Supervisor from company:	J.Wildemast, B.Siegler
Project Duration:	08/2022 - 03/2023
Faculty:	Faculty of Mechanical, Maritime and Materials Engineering, Delft

TU Delft

Offshore Independents Rotterdam

Abstract

Offshore wind energy is undeniably one of the most efficient and rising energy sources in renewable energy industry. Suction caisson jacket is one of the most promising substructures for offshore wind turbines. They consist of a jacket structure combined with a suction bucket on each of its legs. Their unique characteristic of large diameter compared to their small wall thickness, conducts them an object of study, concerning their transportation to the offshore location, as their structural stability should be ensured. The intention of the thesis is to apply a most optimal configuration to sufficiently support the caisson on barge. Prerequisite of that, is to examine the behavior of the caisson, when interacting with the barge during transportation. For this reason, a parametric study is performed, where the stresses and the deformations of the caisson are retrieved and the buckling behavior is examined.

In order to derive the results, a finite element analysis is completed in Ansys. The caisson is designed in the program and its dimensions are selected based on the typical dimensions of a suction caisson, used in an actual project. Besides the geometry design, the meshing process takes place as a next step of the analysis, where the structure is turned into elements in order for the solver to produce a solution. The size of the elements was selected, so that the results are accurate and focused on the area, where the supports exist and the analysis should be more detailed. The boundary conditions are applied in the bottom perimeter of the caisson and they are designed, so as the stiffness of the barge is taken into consideration. The value of the stiffness applied in the supports is based on calculations when the caisson is transported on a typical deck structure. For the loading conditions implemented, their values are derived, based on the load analysis carried out in an actual project. A combination of forces and accelerations act on the caisson. The forces act on the modeled caisson because of the weight of the jacket on top and the accelerations act on both the modeled caisson and the non-modeled jacket, due to the motion of the waves.

Since the subject is based on a parametric study, the change in the parameters concern the supports placed on the base of the caisson. Four(4) supports are placed as a base scenario in the base perimeter of the caisson, in selected segments. In total six(6) cases were examined (A,B,C and D) and compared to the base scenario (case A). In every case the boundary conditions, hence the supports are changed. The supports vary with respect to their length, their location in the base of the caisson and finally the value of their stiffness, according to the placement of the caisson on the barge. More specifically, for cases A to C, the length of the supports is changed, while for case D the location of the supports vary by decreasing the distance of the unsupported area between them. For the final two cases E and F, the stiffness of two out of four supports is increased, in different direction for each of the cases, such that they are considered infinitely stiff.

By performing a linear analysis with the aforementioned inputs, the results were derived for every case of the parametric study and are post-processed in Matlab. The equivalent von Mises stress in the skirt of the caisson is analysed and afterwards the focus is directed in the supported perimeter, where the highest values exist. As a first step the results for the base scenario are evaluated. For the supported perimeter, the directional deformations are derived, based on the cylindrical coordinate system. Therefore, radial(r), tangential(Θ) and vertical(z) deformation is presented for the base perimeter of the caisson. The results showed that the perimeter is deformed outside of the supported segments. Afterwards, the equivalent stress is analysed into its main components: normal stress in vertical(z) and tangential(Θ) direction, and shear stress in θz-direction. From the examination of the stresses, the analysis proceed to the presentation of the axial and bending stress components in tangential(Θ) direction. As a result, it is realized that the most important component, which causes the high stresses in the perimeter of the caisson is the bending stress component and therefore, is the one that should be primarily reduced.

As a following step the results of the parametric study are presented. First of all, the directional defor-

mations are compared for every case (A to D). The results indicated that the deflection in radial(r) and tangential(Θ) direction are reduced when the length of the unsupported area, between the supported segments is also reduced. Furthermore, the equivalent stresses are compared and once again, the trend of stresses in every case follow a similar pattern and the peaks in the supports are reduced when the distance between the supported segments is reduced. Furthermore, in every case the peak values exceed the yield stress limit of the material. In order to understand which parametric case influences more the bending stress component, the comparison for the bending stress component demonstrate that the peaks in the supports are reduced for case D, where the configuration of the supports and the distance of the supported segments is reduced.

As far as the buckling failure is concerned the first 10 modes are derived for the analysis, for every case of the parametric study. The first buckling mode that is taken into consideration in every case, demonstrated that buckling for case A is located on skirt, whilst for case B to D buckling may occur in one of the stiffeners of the lid. Nevertheless, in every case the buckling load factor implies that buckling failure does not have a high possibility to occur for the applied load combination.

For the sensitivity analysis, where the stiffness of the supports is changed, the comparison takes place for cases A, E and F. For these cases, the directional deformations and the equivalent stresses in the perimeter once more are evaluated and show a similar trend. However, the results reveal that the stiffness of the supports based on the barge, do not have a significant influence in the reduction of the values, neither in stresses nor in the deformations. The cases rather show a redistribution of the results in the supported perimeter.

As aforementioned, since in every case the value of the yield limit in stresses is exceeded, a non-linear analysis is performed for a better understanding of the behavior of the caisson, where the peak stresses exist. In this analysis the plastic strains in the caisson are examined, for every case of the parametric study. In every condition, plastic strain appears in a small area of elements near the support. Case C and D owned the smallest values of plastic strain, which are acceptable, and indicated that after yield limit of the material is exceeded and the peak stresses are developed, there will be a redistribution of stresses in the caisson. On the other hand, case A had the highest value and was examined for local and gross yielding. The results implied that even though the value of the allowable plastic strain is exceeded, the local peak stresses of case A are still acceptable.

The final conclusion of the study is that case D is the most optimal configuration for the support of the structure on the barge. Subsequently, the deformations and the stresses developed in the caisson show a similar trend, for every case of boundary conditions. Overall, the design of the grillage should be focused on the reduction of the unsupported area between the supports, rather than increasing the length of the supports.

Contents

List of Figures

List of Tables

List of Abbreviations

SCJ	Suction Caisson Jacket
FEA	Finite Element Analysis
HTV	Heavy Transport Vessel
SPMT	Self-propelled modular transporter
OI	Offshore Independents

1 Introduction

1.1. Literature overview

Over the past few decades offshore wind industry is gaining more and more interest as a renewable source of energy. Many researches were developed in order to examine different foundation types used to support the wind turbines. Among them the suction caissons are a promising foundation recently deployed in offshore wind industry. In detail, the suction caissons consist of a cylindrical bucket (skirt) made of steel, sealed on top (lid) (Figure 1.1). Their distinct characteristic is their large diameter compare to their very small wall thickness. Thus, in order for this shell structure to be successfully placed on barge, the number and configuration of connection points should be selected carefully.

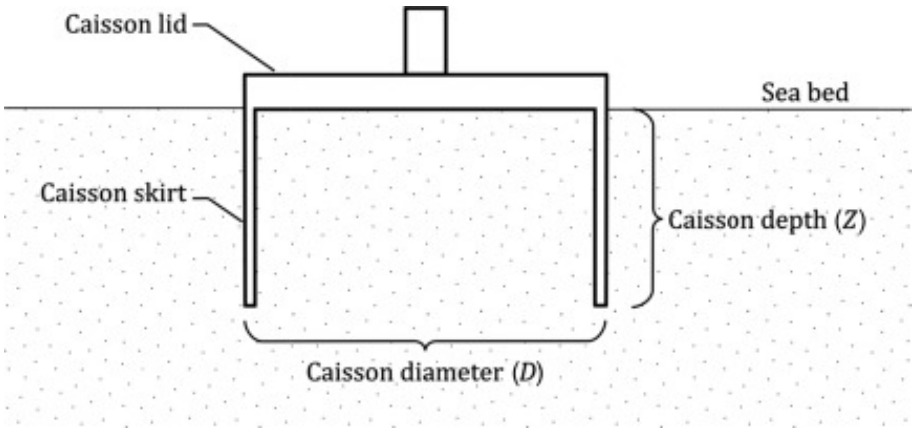

Figure 1.1: Typical layout of a suction caisson (Bhattacharya 2017).

These foundations can be combined with a bottom founded structure like monopile or a jacket, but they can be also used as anchors for floating structures (Houlsby et al. 2005). Their configuration and installation method is already a field of interest for many research studies. However, their transportation method on barge is also something to be considered, as it may become complicated due to their dimensions, which require specific support points on the barge. In general, these foundations can be transported to the offshore location with the help of a barge or a large vessel. The structure is carefully placed on barge and secured, against the motions of the barge, through seafastening connections. The design of grillage and seafastening has to ensure that all loads during transportation of the structure are led into and accommodated by the structure of the barge, without causing overstressing or excessive deformation of the structure or the barge (Tsota 2022).

After the suction caisson jacket (SCJ) are placed on barge, they experience various combinations of static and dynamic loading. The caissons experience the static loading of their own weight and the weight of the jacket that they support. Furthermore, the caissons experience inertia loading due to translational and rotational accelerations (roll, pitch, heave, yaw, sway and surge) caused by motions of the barge and the mass of the jacket. Last but not least, loads due to direct wind and wind heel act to the structure. The loads are distributed to the vessel's strong points by seafastening connections. In seafastening, the points should be selected such as to meet existing strong points on both the caisson

and the barge wherever practicable.

When the suction caisson jackets (SCJ) are transported on the barge, their structural integrity should be ensured. Although there are some alternatives for a better transportation of suction caissons, like wet transportation or changing the design of the caisson. This study is focusing on dry transportation and optimising the configuration of the support points of the caisson on the barge. The difficulty when supporting the caisson lies in the large difference in the dimensions of the caisson (D/t ratio), as it makes the structure flexible, that has to be transported in an already moving barge (in deck and hull), due to the wave motions and accelerations. Furthermore, the caisson is partially supported in the perimeter, so as to leave enough space for both the load-out equipment and the barge to coexist. Thus, the connection points should be given careful consideration and be numerically sufficient, so that the process is successful.

As also explained in detail, in Tsota 2022, the support of the caisson may be performed through steel blocks. The bearing blocks are connected to the grillage and the caisson is placed on top of them. Two shear blocks are welded to the caisson and the grillage and frame the bearing blocks. Each member of the seafastening is intended to undertake a specific load. The weight load of the structure is supported by bearing blocks, while every other vertical load is supported by both the bearing and shear blocks. The shear blocks are also resisting the uplift forces acting on the caisson. All of these, result into investigating which is the most beneficial and economically feasible solution for the number and configuration of support points, in order for the transportation to be completed successfully.

The intention is to apply the most optimal configuration of the support points for the transportation of the SCJ. Prerequisite of that is to examine the behavior of the caisson (i.e. deformations) and the stresses, that the structure experiences during transportation. These can be observed under different support conditions and under a specific loading. The intention is to perform a parametric study by changing the supported geometric boundary conditions of the system, whether that is the number of supporting points or length or the arrangement of the supports. The boundary conditions are selected so as to validate the seafasting method. The study will be carried out performing an ultimate limit state analysis, by applying a standard loading and using the finite element analysis. The main objective is to observe the peak and mean stresses of the caisson during the transportation and how that can be used as a reference to optimize the mechanical boundary conditions, hence the connection points and percentage of the perimeter. Subsequently, conclude the correlation between the stresses and the boundary conditions and examine the deflection of the base of the bucket in any support case. Finally, give recommendations which can be used for a new project for preliminary design purposes (Tsota 2022).

1.2. Research Questions

All of the above regarding the scope of the thesis can be outlined in the following research questions:

- What would be an optimal grillage design?
- What is the behaviour of suction caissons, during transportation when interacting with the grillage and vessel?
- How does the deflection, the stresses and the stress distribution in the caisson's perimeter change when changing the boundary conditions of the system?

1.3. Approach

In order to answer the research questions and attain the objective of the thesis the following approach shall be taken:

- Parametrically model the caisson and boundary conditions in Ansys
- Solve the model for stress and strain distribution
- Vary parameters by changing the percentage of the perimeter's support and the supporting points and repeat the process
- Add stiffness to the model by simulating the supports as distributed springs and derive new stresses by adjusting the stiffness (k) each time in the connection points

As a loading condition, a combination of the nominal weight of the jacket with the barge accelerations is taken into consideration and is applied at the caisson. The loading from the jacket is applied as a vertical and horizontal force and bending moment at the top of the caisson. For the selection of the connection points between the caisson and the grillage the minimum number of points is applied in the beginning, that is four support points, distributed in the supported perimeter. The area of the perimeter, in which the connections can be applied, was selected so that enough space can still remain for both the seafastening connection with the grillage and the load out equipment to co-exist. For the parametric study, the boundary conditions will be examined under three different conditions: changing the length of the supported perimeter, changing the configuration of the support points, changing the stiffness applied in the supports. Support points vary in the available area, thus changing every time the percentage of the supported perimeter. The behaviour under these parameters will be examined each time. For every case the stresses and deformations of the caisson are derived, as well as the buckling behavior of the caisson, focusing in the behaviour of the caisson near the support points.

The stresses will be evaluated in the ULS analysis, where all the factored stresses should be below calculated resistances and the best possible support configuration will be determined based on the case that presents the most favorable stress results and within the limiting criteria. The results will also focus on the trend of the stresses for the different support conditions. The deformations of the caisson will also be assessed, which change according to the applied loading and boundary conditions. Finally, the buckling modes will be determined from the program, in order to check under the specific loading if the caisson is going to buckle and at which parts. These are the most critical results that will determine what is the most optimal configuration for the structure's transportation and will provide a clear insight in the response of the caisson under different support configurations.

,

2
Finite Element Analysis

Finite element analysis (FEA) is a mathematical representation of a physical system comprising an assembly, material properties and boundary conditions. In several situations, product behavior in the real-world cannot be approximated by simple hand calculations. A general technique like FEA is a convenient method to represent complex behaviors by accurately capturing physical phenomena using partial differential equations. FEA has matured and has been generalized so that it can be used both by design engineers and specialists (www.ansys.com 2021). More specifically, it is a computational study which is used to solve partial differential equations in two or three space variables, as is the boundary value problems. The idea behind this technique is to divide the large system in small elements (finite elements), which is achieved by a space discretization in the space dimensions, thus leading to a system of algebraic equations. This is implemented by meshing the entire structure. The applied meshing and size or number of elements usually depends on the complexity of the structure and the different mesh elements can also lead to different results. This method allows for the application of different boundary and loading conditions and different structure materials, even within different parts of the same structure. In order to construct the model, the Ansys program is selected.

2.1. Material Selection

As a first step of the process, the selection of the material used should be input. For the construction of the caisson every part was designed with structural steel S355, based on minimum yield strength of 355 MPa. However the yield strength reduces when thickness increases above 16mm for flat products and hollow sections (NEN-EN-10025 2004). Based on the table 2.1, the yield strength value for the 50mm thickness caisson is amounted to 335 MPa.

Table 2.1: Yield strength of S355 related to thickness

Thickness [mm]	Yield strength [MPa]
t <16	355
16 <t <40	345
40 <t <63	335
63 <t <80	325
80 <t <100	315
100 <t <150	295

To define completely the material properties, it is important to decide what kind of analysis is going to be performed, linear or non linear. In reality, a non linear analysis should be performed to examine accurately the behavior of the structure. Below yield point a linear analysis is just as accurate, as stress and strain have a linear relation. However, when stresses go beyond yield limit then linear analysis is inaccurate. Nevertheless, this does not mean that linear analysis is always unacceptable. In this case study, it is possible for the material to enter the plastic zone, above yield limit. Load cases used play a significant part in this decision. If loads changes in time, then the fatigue cycle and isotropic hardening should be taken into consideration and thus a more complex analysis is required. Since in this case the loads are static and fatigue analysis is not considered, then a linear analysis is also feasible. Furthermore, performing a linear analysis might not indicate how the structure is going to behave after

yielding, it will still provide insight about the trend of stresses when changing the supporting conditions and about the most optimal grillage design. Thus, for simplicity reasons and since it will not result in false estimations, a linear analysis is performed.

Of course, there are some assumptions that follow this analysis. First and foremost, stresses and strains follow always a linear relation and do not follow the actual stress-strain curve. When the stresses exceed the yield limit then the results retrieved for deformations and the values of the stresses are not accurate. Consequently, at this point it will be known that the material will yield and will enter the plastic zone and deformations might also be permanent, but the exact values of them are not known. Nevertheless, it is still possible to determine the results and follow through the scope of the study with the additional advantage of saving a lot of computation time.

2.2. Geometry Design

The first step of modeling the design is to determine its geometric parameters. The design and dimensions of every part of the caisson were selected in order to match typical sizes of a caisson configuration. The project involves a construction of a wind farm in the North Sea, using suction caisson jackets as substructures. It is important to mention that the dimensions of the caissons depend on the loading and soil properties. Each caisson consist of four main parts: skirt, lid, stiffeners and inner tube.

The skirt of the caisson was selected as a cylindrical hollow part with diameter of 10m. The selection was based on the fact that usually their diameter fluctuates between 9.5m-10.5m. Subsequently, the wall thickness follows from the D/t ratio which is ranging usually between 60-200, depending on the under pressure created inside the bucket. For determining the wall thickness in this case the ratio of 200 was selected as a worst case scenario, in order to enhance the difference between the diameter and the wall thickness and make the skirt as a thin shell structure. Thus, a thickness of 50mm was decided. The height of the caisson was designed as 10m, in order to be equal with the diameter. It is suggested that the height of the foundation accounts for usually between 9-13m.

For the lid, the dimensions were chosen based on research of an actual project. Specifically, the lid is of the same diameter as the caisson and has a thickness of 45mm, same as the one in the caissons selected for the wind turbines of the real project. Now the structure resembles the form of a bucket sealed on top, like it should.

In order to create the stiffeners, several aspects where taken into consideration. First and foremost, six stiffeners were chosen in order to enhance the strength of the lid. Nevertheless, with the purpose to simplify the configuration they were represented, included the lid, as a I-section beams. The height of the stiffeners was based on data of realistic project, derived from Offshore Independents (OI), and amounted to 2000mm. The remaining dimensions of each stiffener were selected to meet the criteria of compact sections (class 1) according to EN-1993-1-1 2006. In detail, a vertical force of 30000kN, acting on top and in the middle of the caisson was used for the calculations. The magnitude of the force is an assumption based on the real forces acting on the structure and on the weight of the jacket that is acting on top of the caisson. Since the force is not taken by each of the stiffeners equally, as an unfavorable situation, 40% of the force was applied to one of the stiffeners. When this force is applied directly to the web, the latter should stay under the shear yield limit of $355/\sqrt{3}$, which applies for the selected material of steel S355. With the applied force of 12000kN in the web, the calculations were performed and it was decided that for the web to stay under the shear yield limit, a thickness of 35mm should be used (Appendix A). Nevertheless, the design of the stiffeners was not completed there. In order to enhance the strength of the stiffeners an additional support in the top flange and the web was determined. Specifically, the top flanges are supported by two side beams designed with 35mm thickness each, same as the web. The side beams create an angle of 54.5 degrees, which was estimated by the counterpart beams in the existent project. With this addition, the stiffeners do not undertake the entire loading and hence they do not deform to a large extent, but instead the load is distributed in the skirt and finally in the support points and the barge. The final design of the structure can be seen in Figure 2.1.

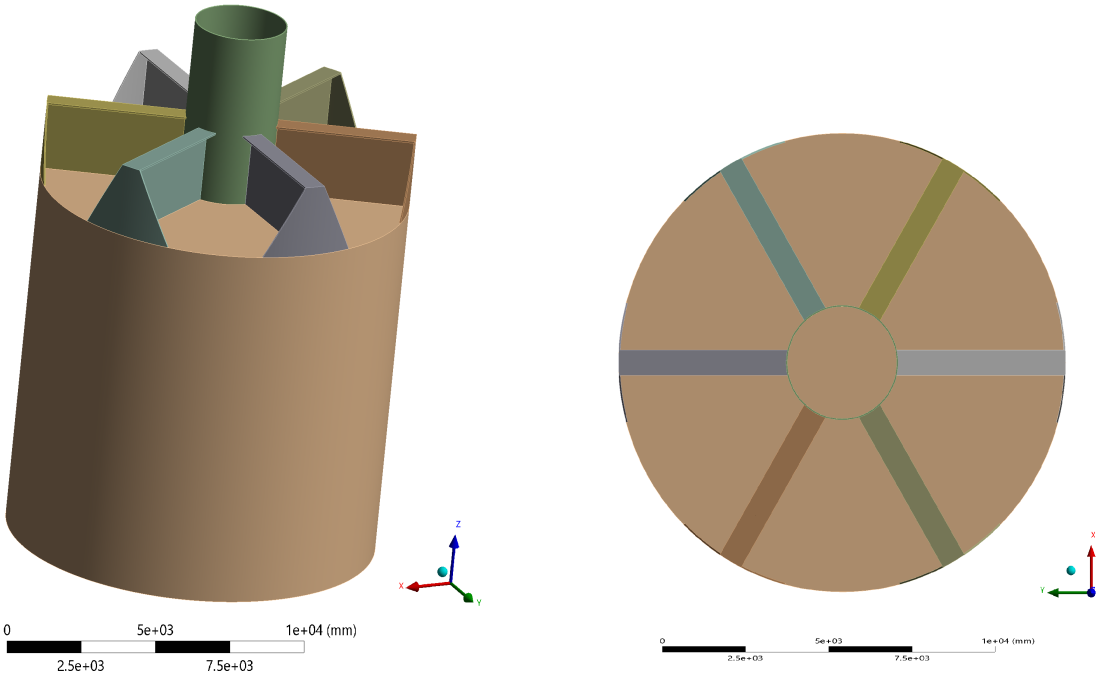

(a) Geometry-side view

(b) Geometry-top view

Figure 2.1: Geometry design of the caisson

At this point, it is important to mention that the modelling could be continued with shell/2D finite elements, since the thickness of the structural parts is relatively small. In order to examine that option, after the design of the solid caisson took place, midsurfaces of each geometrical solid part were created. This turned the total volume design (3D) into a surface elements design (2D). The benefit of completing the analysis only with the surface elements design would be that the meshing procedure is much easier and quicker, and the computation time would be much less, since the program would have significantly less surface area to cover. Indeed, the results were extracted much quicker. However, when boundary conditions were applied, it was realized that the support point could not be simulated similar to reality. This is because the supports should be applied in specific parts of the base surface of the caisson and not in specific points underneath the skirt. In the surface design, as boundary conditions, simple supports were applied in certain points, which led to a small but significant deviation to the results compared to the geometrical solid design. Thus, in order for the simulation to be closer to reality and for the application of support points to be more accurate, the solid elements were selected to proceed the computation.

2.3. Meshing

After the geometry is imported into the Ansys mechanical, the meshing procedure of the structure takes place. Meshing is one of the most important steps in FEA, to perform an accurate simulation of the structure. This process turns the structure into more recognisable volumes called ”elements” (www.ansys.com 2021).These elements contain nodes (coordinate locations in space that can vary by element type), which represent the shape of the geometry. In that way, the solver is able to process the data and produce a solution. The purpose of meshing is to perform the analysis and deliver accurate results with the least computational time. It is important to mention that every part of the caisson is going to be meshed. Thus, it is more manageable to separate it in parts and process each of them. The caisson can be distinguished in the skirt, the lid including the stiffeners and finally the inner tube. The two main aspects of meshing are the meshing size and method.

Each part of the caisson is defined with a specific element sizing. In order to apply the sizing factor, it is necessary to consider which parts of the caisson are of a greater importance for the case study. For these parts, a smaller mesh sizing will be applied and hence a finer mesh structure, which means a high-quality FEA (www.ansys.com 2021). It should be noted that the more the mesh size is reduced, the more the computational time is increased. Since the part of the structure that is the main focus is the support points, it is reasonable to apply a smaller mesh in the bottom part of the skirt. Therefore, for the top part of the caisson, that is the inner tube, the lid with the stiffeners and the top part of the skirt, an element sizing of 200mm is selected. This sizing is used as a starting point in order to provide accurate results but without any particularly detailed resolution and with acceptable computational time. As the analysis progresses along the skirt, the sizing is reduced. Measuring from the bottom of the structure, in 3317mm, the meshing is reduced to 150mm and just above the base of the structure and the supporting points (1776mm from the bottom), which is the main part of interest, the meshing is refined to 100mm (Figure 2.2).

The meshing size is stabilized usually after performing a meshing convergence study. This process involves decreasing the element size and analysing the impact of this in the solution. The change in the meshing size can stop when the results are converged, that is when the dominant values do not differ significantly. Indeed, the convergence study showed that the maximum values of the results in 150mm element size and in 100mm element size were different by only a few decimals. Thus, when the sizing is set to 100mm the meshing can be identified as good regarding the accuracy of the results and the computational time needed to run the program.

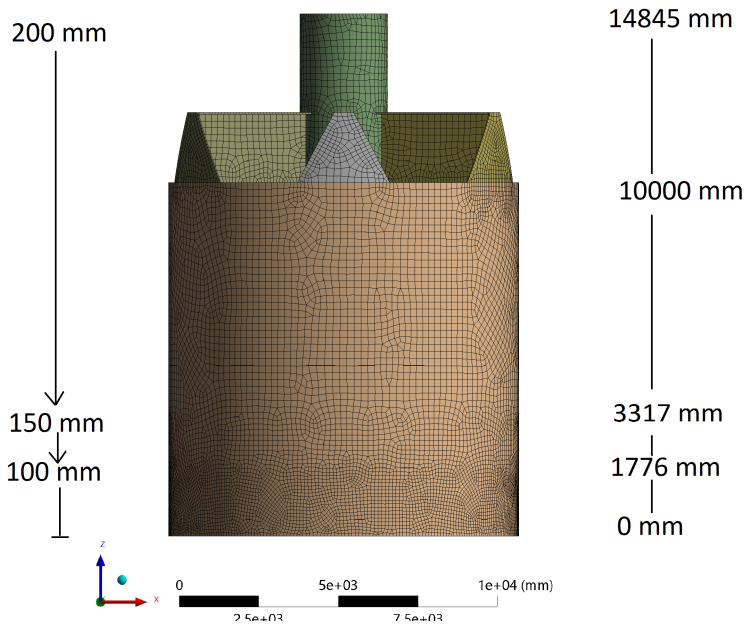

Figure 2.2: Meshing

After the element sizing is applied, the most optimal meshing method should be selected. Several meshing methods can be distinguished:

- Tetrahedal element meshing (”tet”)
- Hexahedral element meshing (”hex”)
- Automatic method
- Sweep meshing
- Hybrid meshing

Usually the most commonly used methods is either one of the first two. Hex elements are known to generate more accurate results than tet elements, however when it comes to more complicated designed structures, tet elements may be the best option. For every part of the caisson hexahedral meshing is used (Figure 2.3). The structure is meshed with 75121 elements and 235505 nodes. This meshing generates meshes composed of deformed cubes (hexahedral) and is often used for simulating some physics (i.e. deformations) because it can improve both speed and accuracy (Ray et al. 2018).Since the solver deals with the full volume of the caisson (solid parts), hex meshing usually has a better numerical efficiency. Hex grids can maintain orthogonal grids in the wall-normal direction and this results in more accurate elements when the angle between faces can be kept close to 90 degrees.

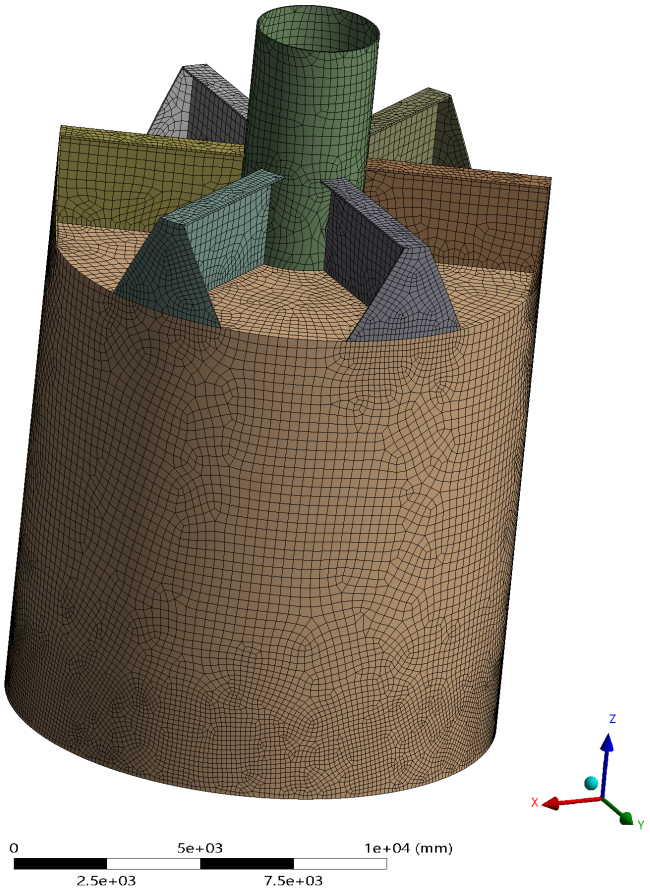

Figure 2.3: Meshing

2.4. Boundary conditions

After the meshing process is completed and the structure is divided in elements in order to be processed, the boundary conditions should be included. It is useful to mention that the top of the caisson is simulated as a free end and no supporting condition is applied. Every condition is applied with respect to the global coordinate system. In order to use the proper boundary conditions, which defines the constraints, the goal is to apply them similarly to the seafastening connections as much as possible. Figure 2.4, shows the seafastening connections of the actual project, in which the boundary conditions should be complied with.

(a) Shear and Bearing plates for seafastening

(b) Caisson with seafastening connections

Figure 2.4: Seafastening connections on actual project

In order to recreate the support points, the surface area of the base of the caisson, was divided into 44 parts of equal length (Figure 2.5). Each segment is amounted to 8 degrees arch angle and 698mm arch length, except one. Segment 11, is larger by almost 300mm (1040mm length in total), because of the automatic division of the perimeter performed in Ansys. However, this segment is used in 2 out of 4 examined cases and will not influence the results or the comparison at the final evaluation. Every support point corresponds to one boundary condition, which is applied at one or more segments.

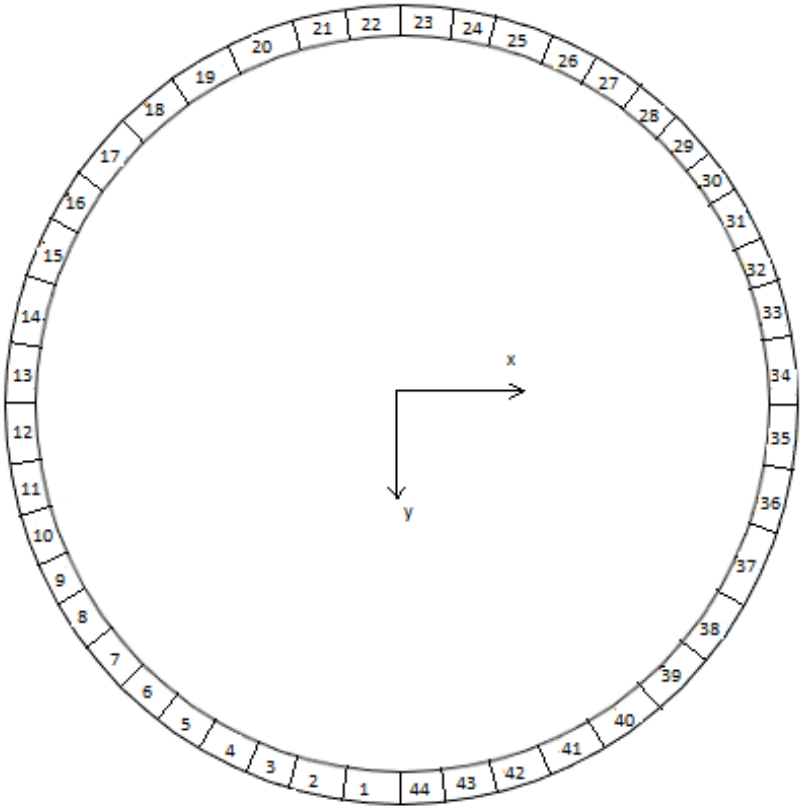

Figure 2.5: Division of the perimeter in segments

As a first application of the supports, the caisson was supported at fixed points and thus creating an infinite stiff system. Each boundary condition was applied as fixed support in one segment. However, this does not take into account the flexibility of the system that supports the caisson (barge, grillage, seafastening). In order to change that and add stiffness to the system, for each support three conditions were included in every segment, according to the cylindrical coordinate system (figure 4.1). As can be also seen in the figure 2.6, where support A is presented, three radial springs in r-direction (kA1, kA2, kA3) and one tangential spring in Θ-direction (kA4) is applied, as well as one elastic support in vertical z-direction (kA5) (Table 3.1). In horizontal direction, the system did not allow for an application of the distributed springs, therefore in order to apply the sufficient stiffness, radial and tangential springs were applied in different points across the length of the supported segments. The radial springs where applied at the two ends and the middle of the supporting segment area each time, providing distributed load transfer. The tangential spring is applied at the middle of supporting centre and the vertical elastic support is evenly distributed over the segment area, where the constraints are applied, automatically by the software.

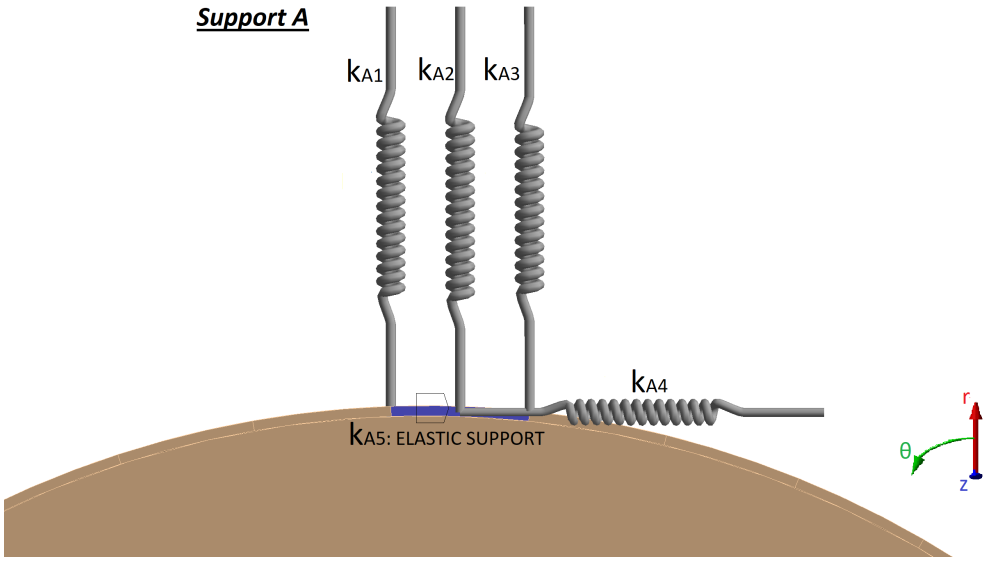

Figure 2.6: Definition of elastic constraints in one segment as appeared in Ansys

The stiffness was estimated based on the assumption that the SCJ and hence the caisson is transported by a typical deck structure of an Heavy Transport Vessel (HTV). The complete vertical force was divided between the four(4) grillage beams that support the caisson (Figure 2.7). Each grillage beam is supported by 2 web frames, as can be seen in the figure, so 1 web frame is loaded by half of the grillage load. A typical web frame is assumed to be supported by vessel's shideshell and longitudinal bulkheads. Each web frame is simple supported over longitudinal members. The deflection of a web frame was calculated and from that the equivalent vertical spring stiffness (Appendix A.2). To take into account the horizontal stiffness, knowing that the vessel deck is much more stiff in plane of the deck, the value of the vertical stiffness is multiplied by 10. The grillage beams are assumed infinitely stiff at the end constraints. After all, the stability of the system should be ensured and especially in the support points, which should not have any perceptible deflection

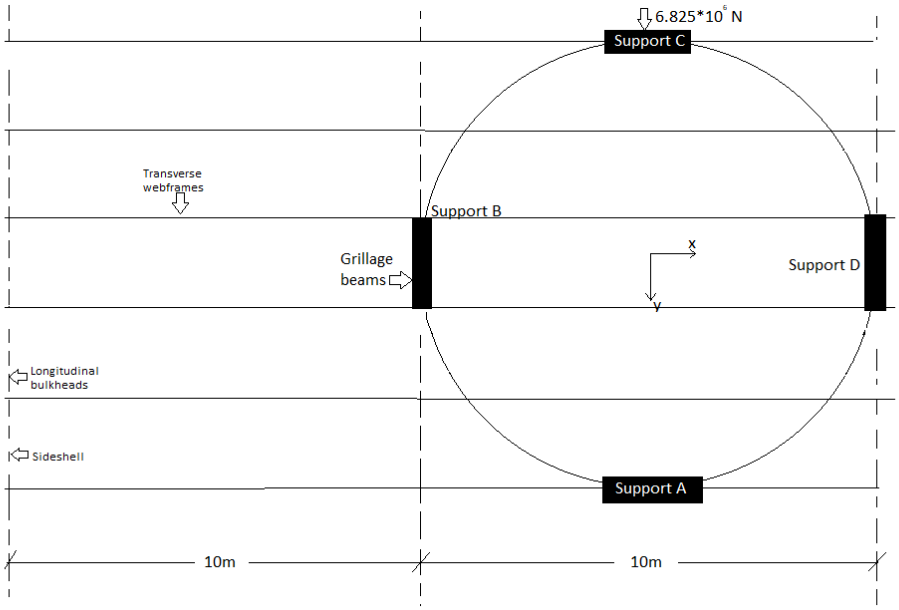

Figure 2.7: Caisson placement on top of grillage deck

2.5. Loading conditions

For the loading conditions, there are different forces and accelerations acting on the caisson, both cases applied with respect to the global coordinate system. Usually, in order to obtain the loads acting on the caisson and determine the most dominant ones, a loading analysis should take place. In this case the loads were supplied as well by OI, as a data based on an existent project. The loads are determined such that their values are similar to those derived from the structural analysis of the actual project. The loads, selected for this case study are considered factored, where the factors are applied according to DNVGL-ST-N001 2018. The reason behind this decision, was to focus the research completely in the behavior of the caisson after the loading is applied and not in the calculation of the forces acting on it. The weight of the jacket structure and the heave load are applied as one vertical and one horizontal force of Fz= -25000KN (heave translation) and Fy=6000KN (sway translation) respectively, in the center and on top of the caisson, where realistically, the caisson is connected to one of the legs of the jacket and is conservatively regarded in this study as a free end, with no boundary conditions applied. Because of the height of the jacket, moment is also developed and act at the same location, about x-axis (rolling motion), causing longitudinal rotation with the value of Mx=12000 KNm. The accelerations due to motion of the waves, act on the center of mass of the caisson and are applied as two values of heave acceleration over z- and sway acceleration over y-axis and were accounted for az=-13 m/s^2 and ay=7 m/s^2 (Figure 2.8). It should be mentioned that in reality the wind loading should also be included. However, for simplification reasons it was not considered in this case study.

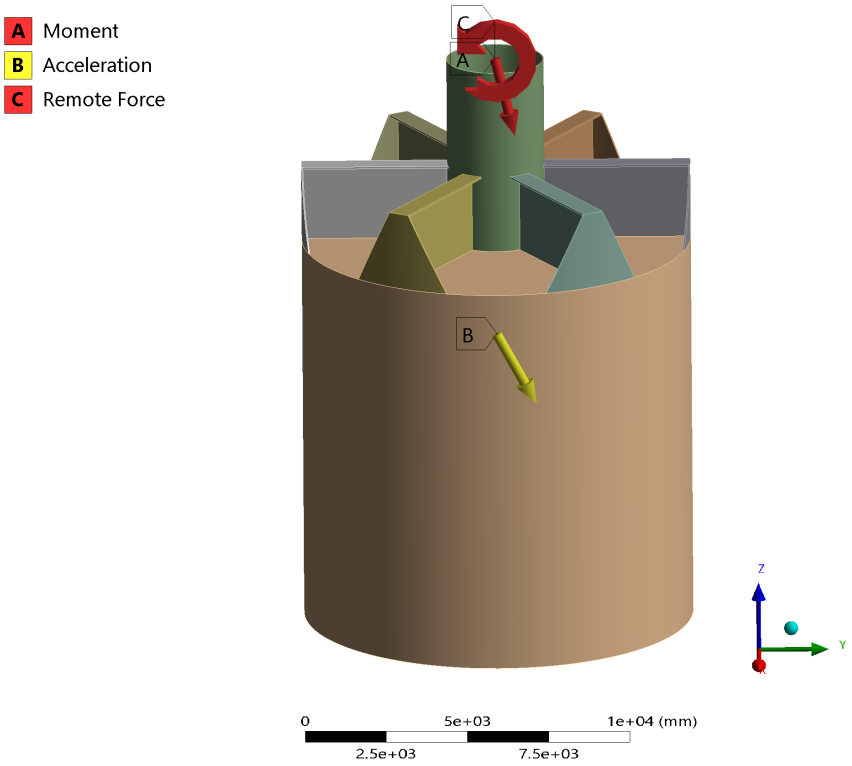

Figure 2.8: Application of loads in the caisson

The directions of the applied loads were determined in order to evaluate the different support cases under the most critical loading combinations. In order to determine the combinations for the dynamic loading, the transportation inertia standard loads for default motions are combined as shown in table 2.2. However, through careful consideration it is concluded that the most dominant load case is the first one, where gravity acts on the same direction as the acceleration and positive roll moment is causing positive sway motion.

Table 2.2: Load combinations

Load combinations		Fz [KN]	Fy [KN]	Mx [KNm]	ay [m/s^2]	az [m/s^2]
1	***- Heave + Roll***	-25000	6000	12000	7	-13
2	***- Heave - Roll***	-25000	-6000	-12000	-7	-13
3	***+ Heave + Roll***	-12692	6000	12000	7	-6.6
4	***+ Heave - Roll***	-12692	-6000	-12000	-7	-6.6

As can be observed, gravity (9.81 m/s^2) acts in the same direction as the heave acceleration (negative z-direction). Hence, the two values are added and the values of heave force acceleration in table 2.3 is derived. The rolling moment acts on positive x-direction, creating positive roll and causing a positive force in y-axis and creating a sway motion (Table 2.3). The forces appeared on the table, represent the internal loads from the jacket leg, which is not modelled, to the modelled caisson. The accelerations act in reality both on the modelled caisson and the non- modeled jacket.

Table 2.3: Applied loads

Forces			**Accelerations**	
Fz [KN]	Fy [KN]	Mx [KNm]	az [m/s^2]	ay [m/s^2]
Heave	*Sway*	*Roll*	*Heave*	*Sway*
-25000	6000	12000	-13	7

2.6. Force equilibrium check

In order to assure that the boundary conditions and definition of the loads are applied correctly, an equilibrium of forces check is performed to observe if the applied loads match the reaction forces. This check has as an objective to verify the results of finite elements analysis and to ensure that the analysis has run smoothly. The check was completed for the first case scenario of 4 supports and single segment per support. From the table 2.4 can be clearly seen that there is little to no differences between the reaction and the applied forces, which were calculated with respect to the global coordinate system, therefore the boundary and loading conditions are successfully applied. For the calculation of the applied load, all the forces and accelerations were considered and included in the calculation.

Table 2.4: Equilibrium of reaction and applied forces

Load Cases	Fx [KN]	Fy [KN]	Fz [KN]
Support A	-74	-1189	15017
Support B	384	-2586	7038
Support C	-34	-775	-2365
Support D	-275	-2708	7648
Total reacted load [KN]	-0.008	-7259	27338
Total applied load [KN]	0.006	7259	-27338

3
Parametric Study

In order to examine different supporting conditions under which the caisson could change its behavior and finally observe which is the most favorable, a base scenario was first established. First and foremost, in order to select the segments in which the boundary conditions will be applied, there should be ensured that enough space will remain at the same time for the loadout operation. Considering that the loadout operation will be performed through trailer, which will be placed underneath the base of the caisson, the segment seen in the figure 3.1, where selected to remain as a reserved path for any SPMT operation to be performed. The reserved path was selected with respect to the typical dimensions of an SPMT trailer unit, which sets a distance width of 1400mm. Therefore, three segments of total width of almost 2000mm will apply to the requirements.

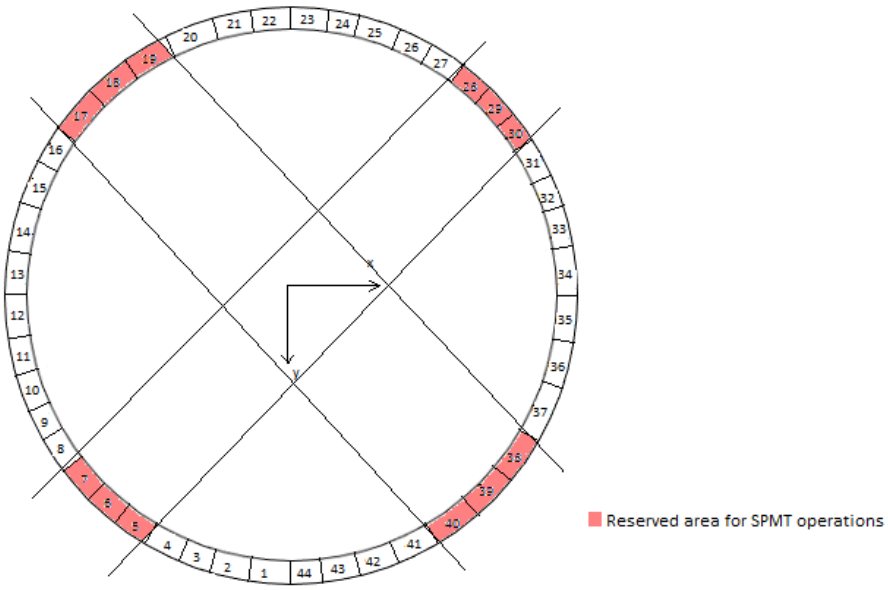

Figure 3.1: Reserved segments in the base of the caisson

In the remaining area the restraints can be applied in any of the segments. For the base scenario the minimum number of allowable supports were selected. Four supports were applied, each of them occupying one segment (Figure 3.2).The location of the supports, and hence the remaining space for SPMT operation, was picked, in order to allow for at least one segment (i.e. Segment 1) to experience the full load (Fy) and observe the behavior in the support. In table 3.1, there is an overall reference to the application of the supports, in case A as an indication, and similarly applied in every other cases, A to D, of the parametric study. Every time the supports change between the allowed segments and the results should be comparable to one another.

Table 3.1: Types of supports in every supported segment-case A

Supported segments	Types of springs					
	R (radial direction)		*Θ (Tangential direction)*		*Z (Vertical direction)*	
S1	3 springs	$9 \cdot 10^6\ N/mm$	1 spring	$9 \cdot 10^6\ N/mm$	1 Elastic support	$9 \cdot 10^5\ N/mm$
S12	3 springs	$9 \cdot 10^6\ N/mm$	1 spring	$9 \cdot 10^6\ N/mm$	1 Elastic support	$9 \cdot 10^5\ N/mm$
S23	3 springs	$9 \cdot 10^6\ N/mm$	1 spring	$9 \cdot 10^6\ N/mm$	1 Elastic support	$9 \cdot 10^5\ N/mm$
S34	3 springs	$9 \cdot 10^6\ N/mm$	1 spring	$9 \cdot 10^6\ N/mm$	1 Elastic support	$9 \cdot 10^5\ N/mm$

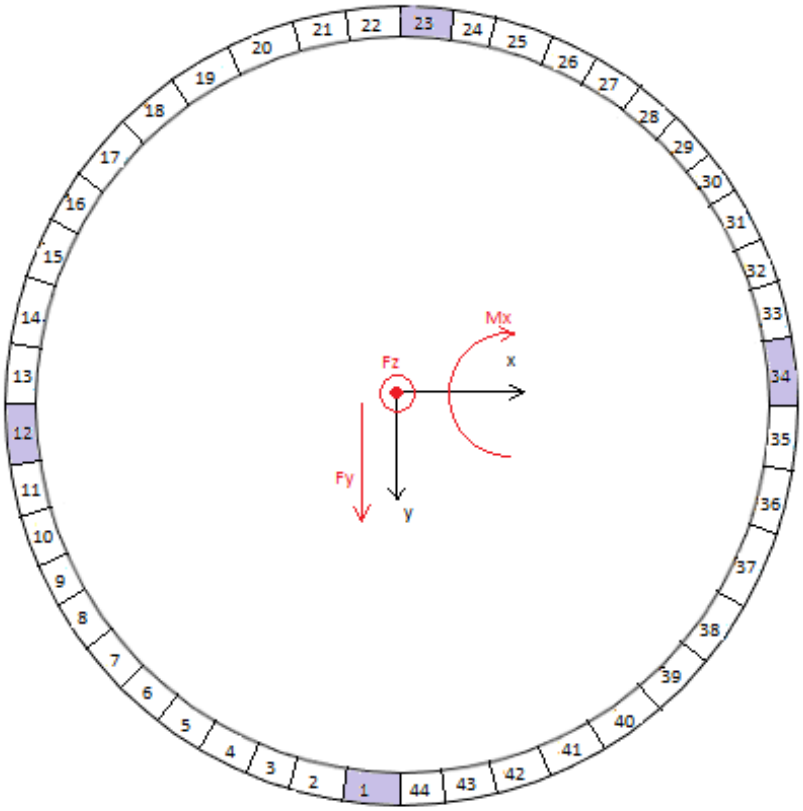

Figure 3.2: Base scenario supports

For the parametric study, the cases were selected by changing the percentage of the perimeter that it was supported each time based on different parameters. These parameters are subjected to changing the length of the supported segments or the configuration of the supports or finally the stiffness of the supports. In total 6 cases were examined and compared to each other as can be also seen in table 3.2.

Table 3.2: Cases examined in the parametric study

Parameters		
Supported segments	***Percentage of supported perimeter***	***Name***
1-12-23-34	9%	A
1/44-12/13-22/23-34/35	18%	B
2/1/44-11/12/13-22/23/24-33/34/35	36%	C
2-11-14-22-25-33-36-43	18%	D
1/23 (Fix supports)-12/34 (Elastic supports)	9%	E
1/23 (Elastic supports)-12/34 (Fix supports)	9%	F

At first the study is focused to examine the influence of the length of each support in the results. The length of each support was increased by a segment every time (Figure 3.3), in cases B and C. The number of segments, which are supported, are identified for every case in this figure. This decision leads to 2 segments per support, and 18% of the perimeters supported, and subsequently to 3 segments per support, and 27% of the perimeters supported. Furthermore, a change in the configuration was also examined, which again corresponds to 18% of the perimeters supported, however by keeping a distance between the segments. Since cases A to D refer to the change of the stiffness of the barge, they are selected for the comparison between them in the parametric study.

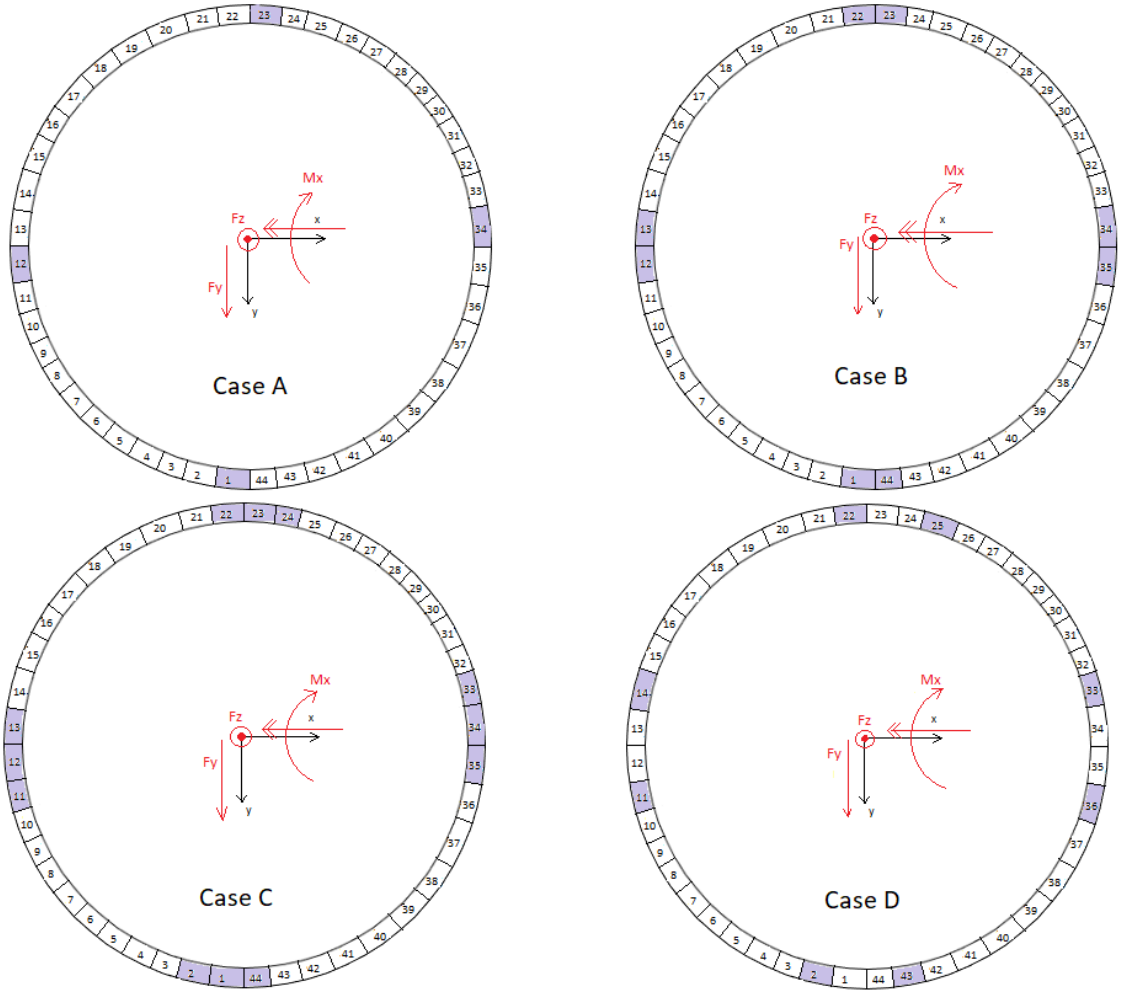

Figure 3.3: Parametric study cases

Nevertheless, by taking into account that the caisson will be placed on top of the barge it is useful to examine also it's position. More specifically, considering figure 2.7, if the grillage beams are placed on top of the bulkheads (i.e. Support B and D in the aforementioned figure), the stiffness in vertical direction is much larger there, almost infinite, compared to the rest of the deck. In these supports instead of including the stiffness, they could be simulated as fix supports. Thus, cases E and F were created by changing each time the direction of fix supports. In case E, segments 1 and 23 were considered as fix (infinite stiff supports) and the rest remain with the same stiffness ($9 \cdot 10^6\ N/mm$ in radial and tangential and $9 \cdot 10^5\ N/mm$ in vertical direction) , while in case F, segments 12 and 34 were considered as fix (Figure 3.4). In the former the supports receive the total load (Fy) and moment (Mx) is divided between the two fix supports, while in the latter the fix supports are located in the neutral axis of the moment

(Mx). An overall description of the application of the supports in cases E and F is also presented in table 3.3. Therefore the cases A, E and F are compared at a second stage considered as a sensitivity analysis that regards the stiffness of the barge.

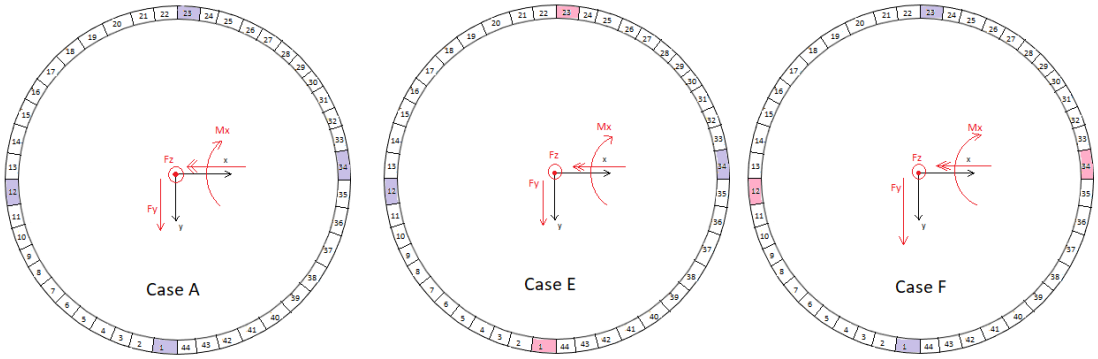

Figure 3.4: Sensitivity study cases

Table 3.3: Types of supports in every segment-cases E and F

Case E			
Supported segments	**R (radial direction)**	**Θ (tangential direction)**	**Z (Vertical direction)**
S1	-	-	Fix support
S12	3 springs | $9 \cdot 10^6\ N/mm$	1 spring | $9 \cdot 10^6\ N/mm$	1 elastic support | $9 \cdot 10^5\ N/mm$
S23	-	-	Fix support
S34	3 springs | $9 \cdot 10^6\ N/mm$	1 spring | $9 \cdot 10^6\ N/mm$	1 elastic support | $9 \cdot 10^5\ N/mm$
Case F			
Supported segments	**R (radial direction)**	**Θ (tangential direction)**	**Z (vertical direction)**
S1	3 springs | $9 \cdot 10^6\ N/mm$	1 spring | $9 \cdot 10^6\ N/mm$	1 elastic support | $9 \cdot 10^5\ N/mm$
S12	-	-	Fix support
S23	3 springs | $9 \cdot 10^6\ N/mm$	1 spring | $9 \cdot 10^6\ N/mm$	1 elastic support | $9 \cdot 10^5\ N/mm$
S34	-	-	Fix support

4
Results and Discussion

After the completion of the analysis of the parametric study in Ansys, the proceeding step is the evaluation of the results. In order to observe the behavior of the structure under the different boundary conditions, the caisson was examined for its stresses, total and directional deformations and eigenvalue buckling. These modes were selected for evaluation since they are the most dominant parameters in the response of the structure and might lead to failure. Every result will be presented in the following sections after a post processing in Matlab, which served in presenting clearly and comparing the results. As an important reminder it is useful to mention that the results exist only under the specific applied loads. During the lifetime of the transportation the caisson experiences different load combinations and load cycles, thus it is influenced also by fatigue and the results may differ. Nevertheless, the results will provide a clear insight in the behavior of the caisson under this critical loading. For the deduction of some results, a cylindrical coordinate system was created (Figure 4.1). The origin of the coordinate system is created automatically by Ansys.

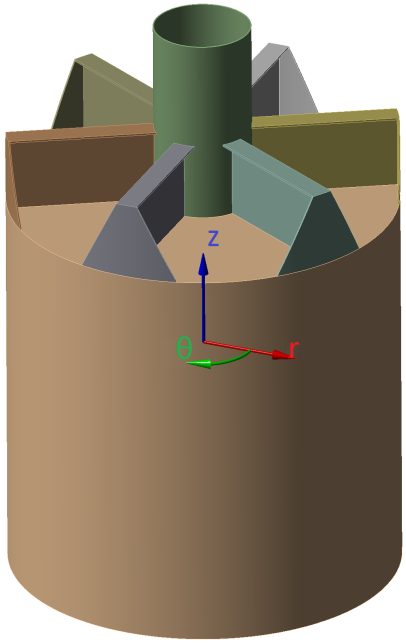

Figure 4.1: Cylindrical coordinate system

4.1. Equivalent von Mises stress over the skirt

The first results of the study deal with the retrieve of the equivalent von Mises stress for the whole caisson and subsequently focusing on the supported area. This value was selected for evaluation, not only to determine whether the material will yield or fracture, under the applied load, and hence whether the supports are capable of withstanding the loads, but also as a first step to the stress analysis that is performed. Furthermore, the values of the results are linked to the meshing size. If the meshing size is increased, then the values might be different by a lot, according to the element size.

Figure 4.2 and 4.3, represent the development of the stresses over the length of the skirt. The figures illustrate cases A and B, in which the distribution of stresses is representative for all cases. The representation of the results is scaled in a such way so as to focus on the allocation of stresses in the caisson and not on the actual values. As can be clearly seen, the image, almost everywhere in the surface of the caisson the stresses follow a similar value (in average of 100 MPa), whilst in the bottom perimeter, very high spikes in the values of the stresses appear in the location of the supports, proving that this indeed should also be the focus of the research in order to analyse the stresses. At 10m height it can be observed that there are also some spikes, much smaller than those in the base of the caisson, however these appear in locations where the stiffeners of the lid are. This shows a load accumulation at the stiffeners, which is transported from the top of the lid, where is applied through the stiffeners in in the rest of the skirt and finally in the supports.

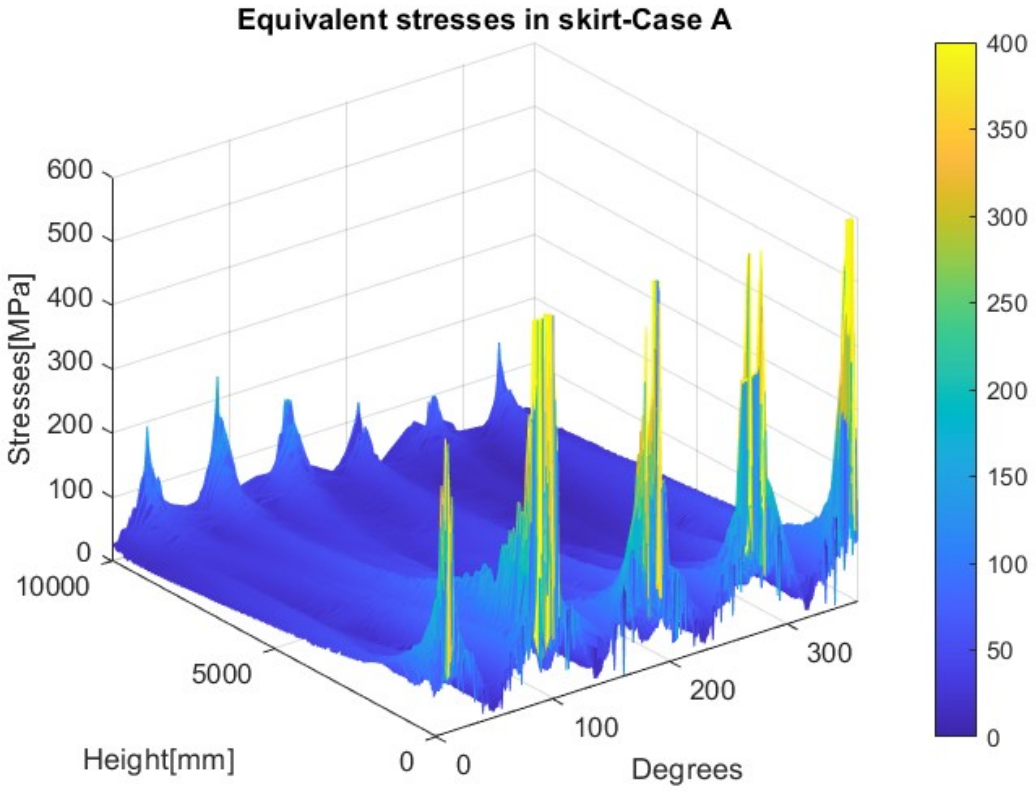

Figure 4.2: Equivalent von Mises stresses in skirt-case A

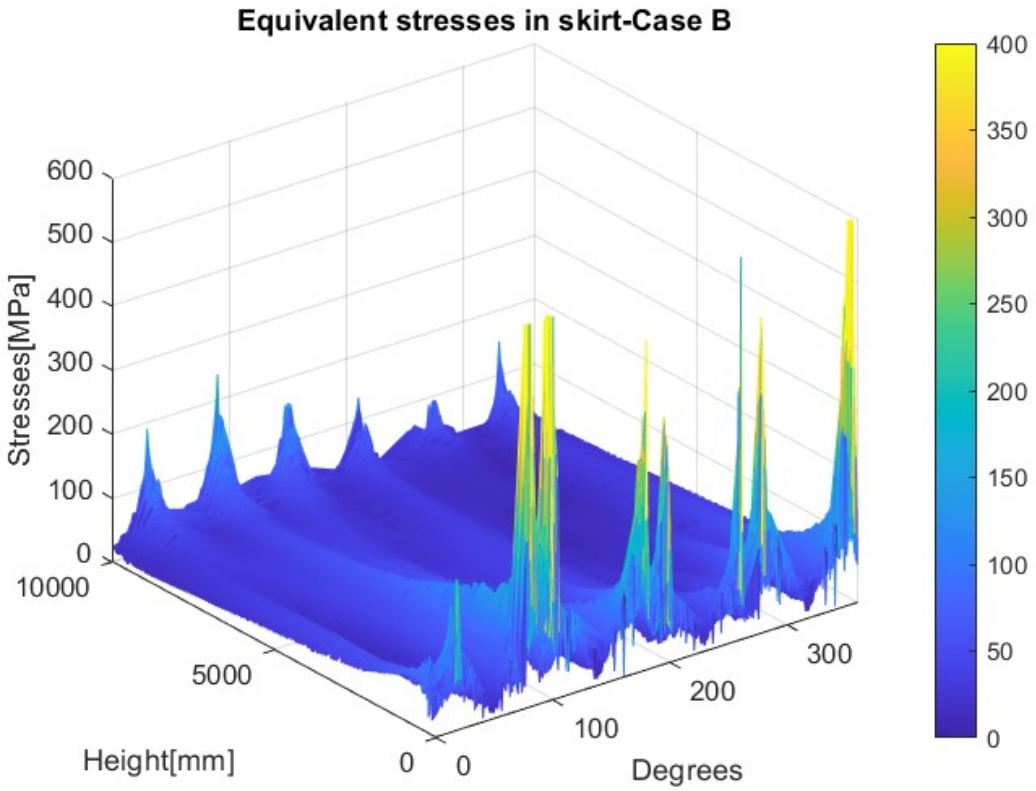

Figure 4.3: Equivalent von Mises stresses in skirt-case B

For further explanation, figure 4.4 represent the development of stresses across the skirt for case A but by creating a cross section in half of its length. As indicated in this figure, the peaks on top in the stresses imply the presence of the stiffeners on the lid and the curves in 5000mm correspond to the supports. This figure show the flow of the stress from the top of the skirt towards the supports. More specifically, the second and third stiffener, which are located at 90 and 150 degrees respectively, contribute towards the second support which is located in 90 degrees. The stresses from these stiffeners seem to be converging towards this support, thus resulting as a first impression that in this support, higher stresses will be developed. On the opposite side, at 270 degrees where there is also a support, even though the stresses are similarly distributed from the stiffeners, the value of stresses in this support would be much less.

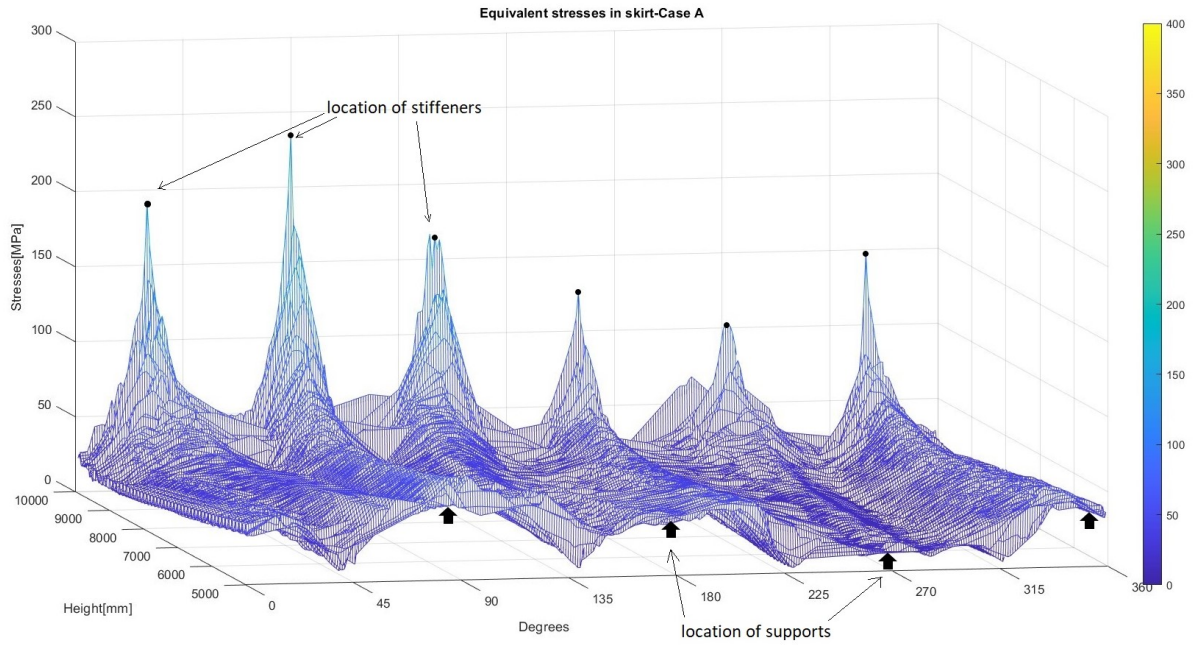

Figure 4.4: Equivalent von Mises stresses in skirt-cross section

Finally, figure 4.5 , shows the isolines of stresses over the height of the skirt. As observed, the contour lines specify the stresses with the similar values, which are concentrated near the perimeter of the skirt and specifically close to the supports, whilst in the rest of the height they are not even represented in the figure.

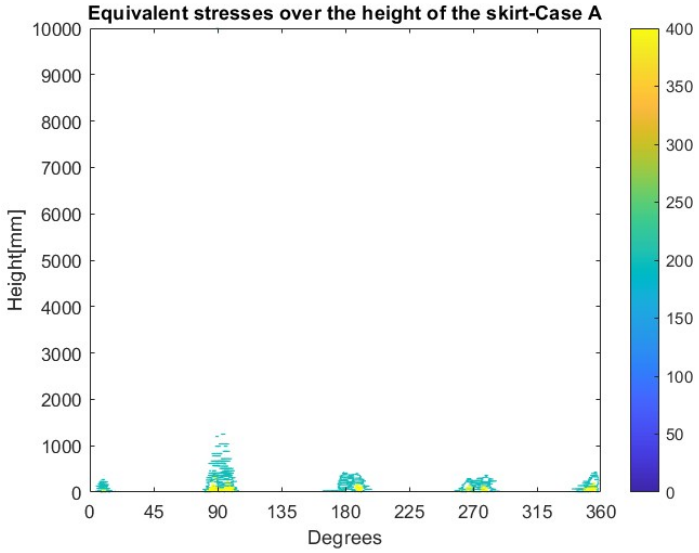

Figure 4.5: Equivalent stresses distribution over the height of the skirt

4.2. Base Scenario

Before the comparison of the cases and the analysis are developed further, it will be beneficial to observe what happens to the base scenario. As aforementioned the base scenario or case A, will be analysed based on the deformations, the stresses and the buckling. As a first step it is useful to investigate how the perimeter of the caisson deflects in every direction. In figures 4.6 and 4.7, the deformations in radial(r) and tangential(Θ) direction appear respectively. As can be observed from the figures in radial deformation the perimeter tends to deform between the supports, both in and out of plane of the structures initial form, on contrary to tangential deformation, where between two supports, the perimeter seems to deform only in one direction. Figure 4.7, illustrate two negative and two positive deflection in the perimeter, consecutively. This may be due to the direction of the moment Mx, causing distortion towards one side of the caisson. In the supports, the deformation in both directions, appear to be zero (0), which indicates that the application of radial and tangential springs is effective and their value is high enough to prevent movement in any direction at the support points. In radial deformation the maximum value is of +/- 30mm, whilst in tangential deformation is much less, with a value of +/- 13mm. In both cases though the values are much less than the thickness of the caisson. In figure 4.8, the vertical deformation in the base perimeter is illustrated. The supports are deformed as well in this case, as the deflection of the deck, as modelled by the elastic supports. The figure illustrates that most of the supports and the base of the caisson shows a negative deflection (downward load area), which indicates that this area is in compression. Only a small part of the perimeter, segment 23 is in tension, with positive deflection values just above 0 (uplift area). This is reasonable considering the application of loads and especially Fz, which is applied downwards in the caisson.

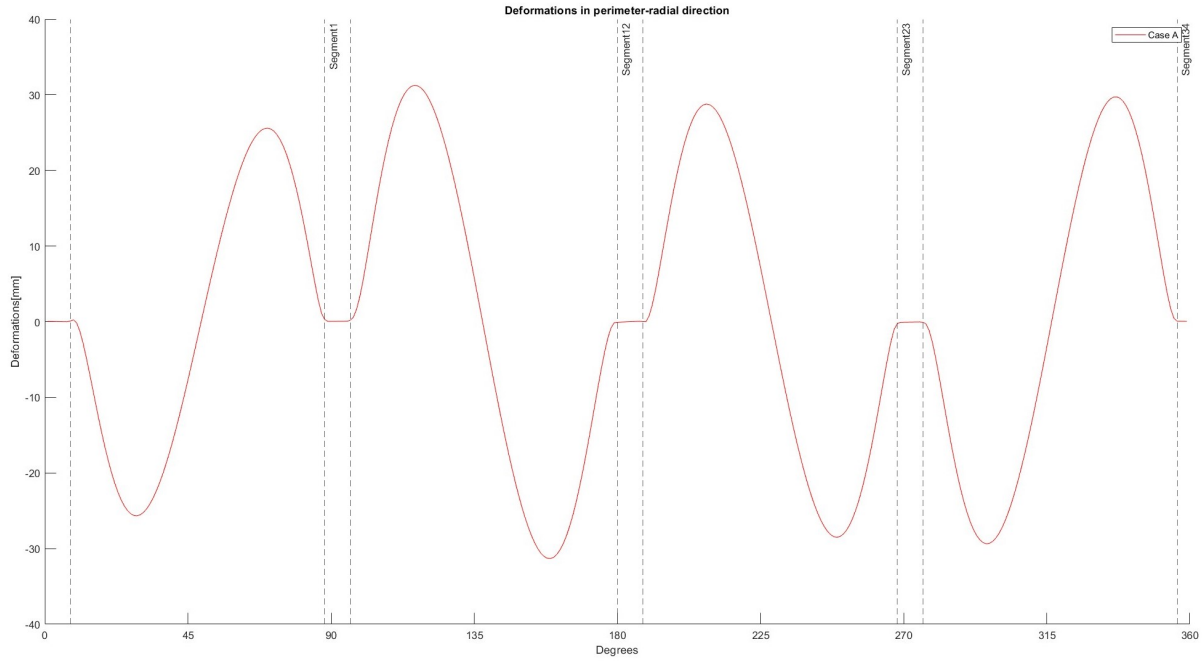

Figure 4.6: Radial deformation in base of caisson-Case A

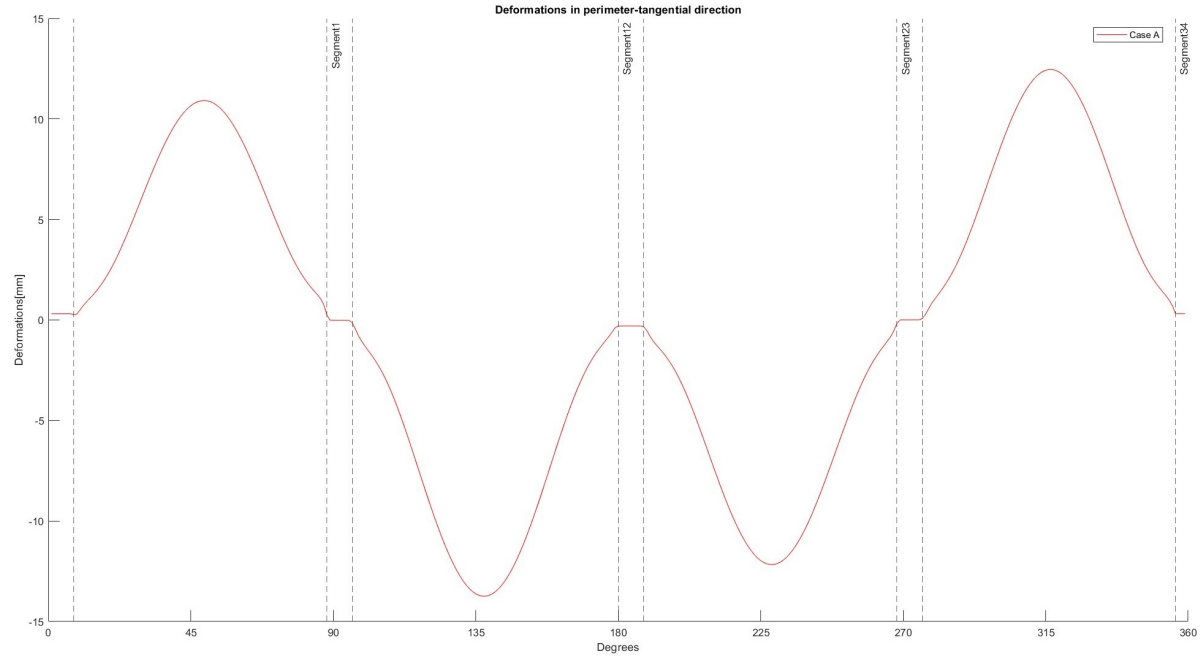

Figure 4.7: Tangential deformation in base of caisson-Case A

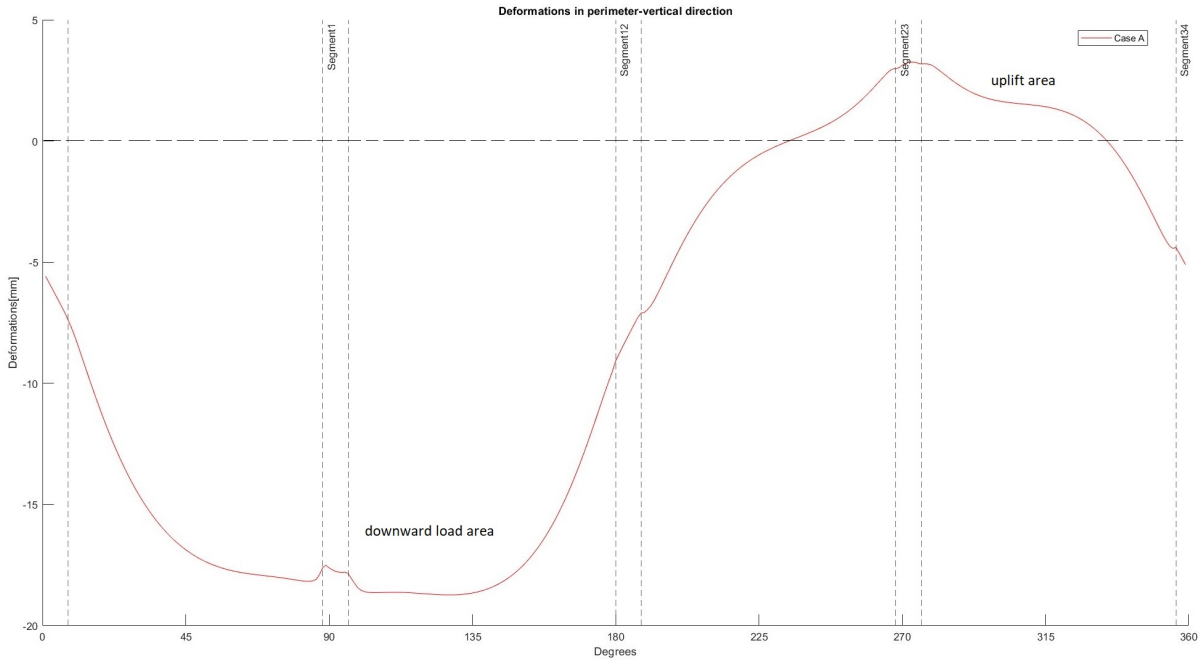

Figure 4.8: Vertical deformation in base of caisson-Case A

After the deflection is analyzed, stresses are also an important factor of the behavior of the caisson. Figure 4.9 demonstrates the equivalent von Mises stress in the caisson's base perimeter. As a first impression it is observed that the stresses show a homogeneous distribution throughout the perimeter around 100MPa, except at the edges of the supports. There, the stresses show a very high peak due to the distribution of force from the caisson to the supports. In order to evaluate whether the yield limit

is exceeded, according to DNVGL-RP-C208 2019, the values of global peak stresses should be compared to the global stress limit as following:

$$\frac{yield\ limit}{material\ factor} = \frac{335}{1.15} = 309\ MPa$$

The peaks at the edges of the supports show very large values, much higher than the calculated stress limit, with the extreme value appearing in segment 1. This shows that the yield strength is exceeded and plastic zone is reached. Some of the deformations which are developed can be permanent and non reversible.

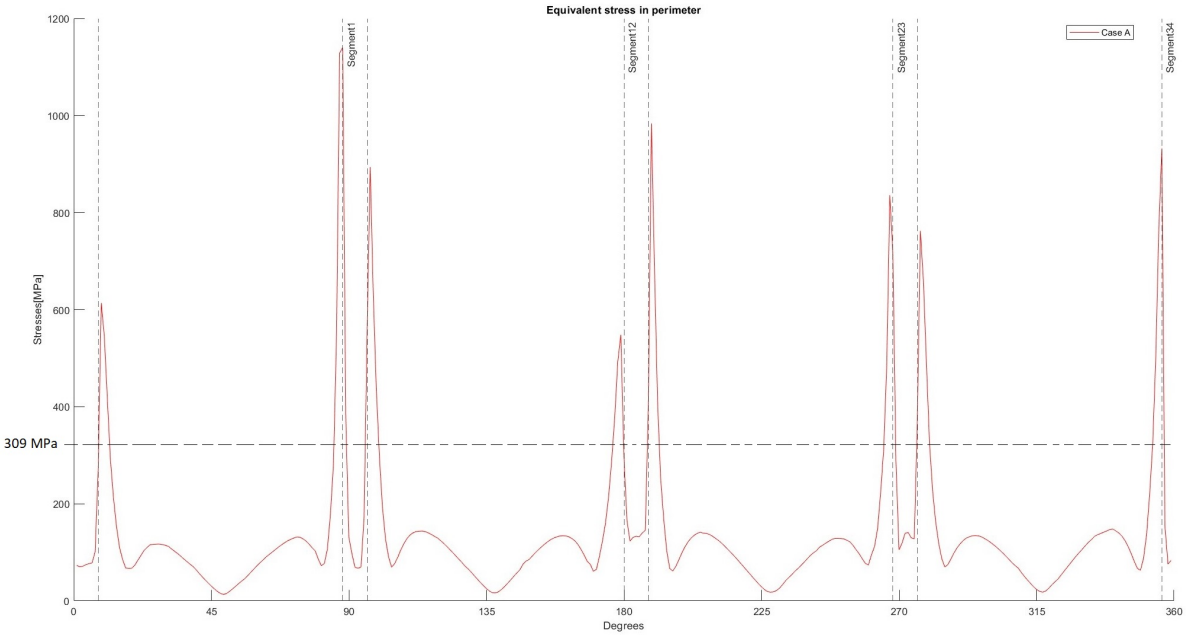

Figure 4.9: Equivalent stress in base of caisson-Case A

Since the equivalent stress is assessed, the value could be analysed at its components. Thereafter, the most important components are retrieved with respect to the cylindrical coordinates system. Normal stress in vertical (Z) and tangential (θ) direction (σz and σθ) and Shear stress in ΘZ direction (τθz). Figures 4.10, 4.11, 4.12 illustrate the aforementioned stress components as developed in the perimeter of the caisson. The purpose of this presentation of the figures, is to identify the most important component, which influences the equivalent stress. The figures reveal that the most important component is normal stress in tangential direction (Figure 4.11). This becomes noticeable based on the von Mises formula, which has been examined (EN-1993-1-6 2006). As observed the normal stresses in tangential direction show peaks at the same locations as the equivalent stresses and follow a similar distribution pattern in the supported perimeter as well. Furthermore, by comparing the components the normal stress in tangential direction owns the largest values, which clearly influences the high peaks in equivalent stresses. It is noted as well that in σz and σθ charts, there is a change in the values in the supports, from negative to positive. This is an indication of the presence of bending moment, which influences the normal stress in the supports.

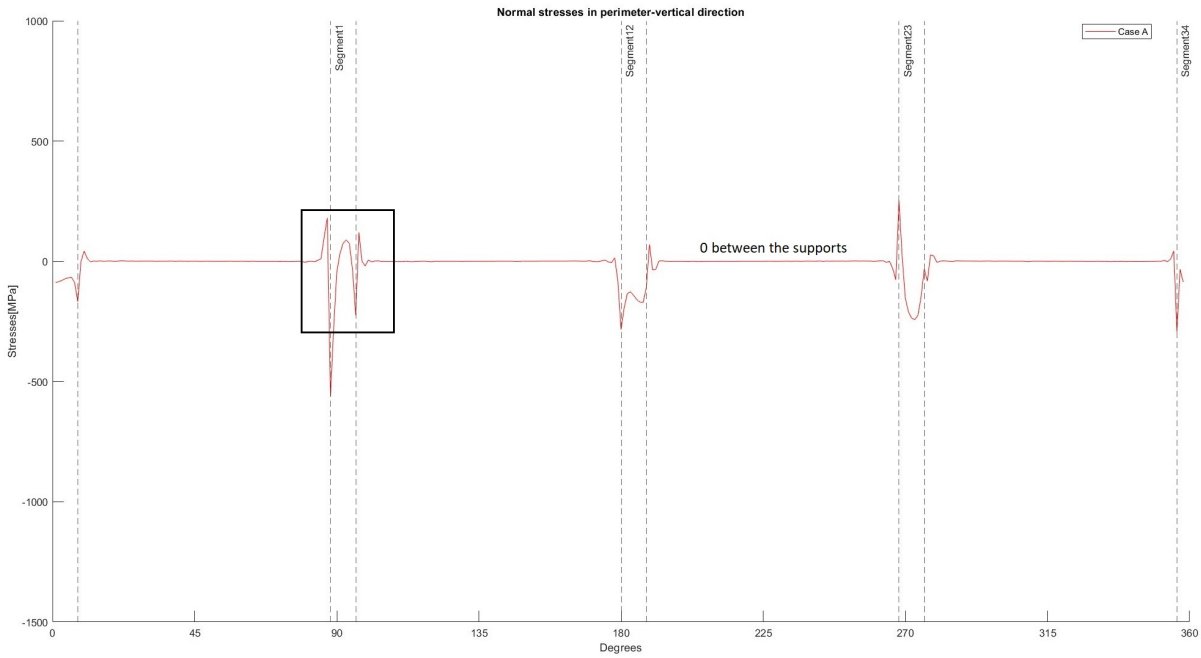

Figure 4.10: Normal stress in base of caisson-vertical direction-Case A

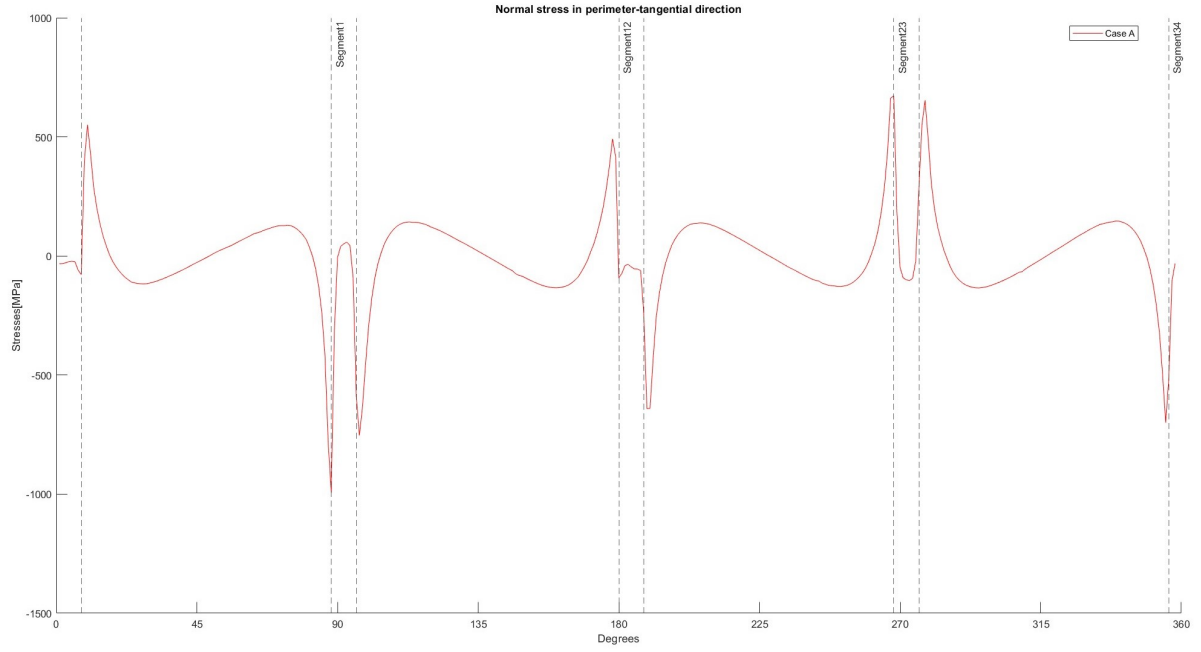

Figure 4.11: Normal stress in base of caisson-tangential direction-Case A

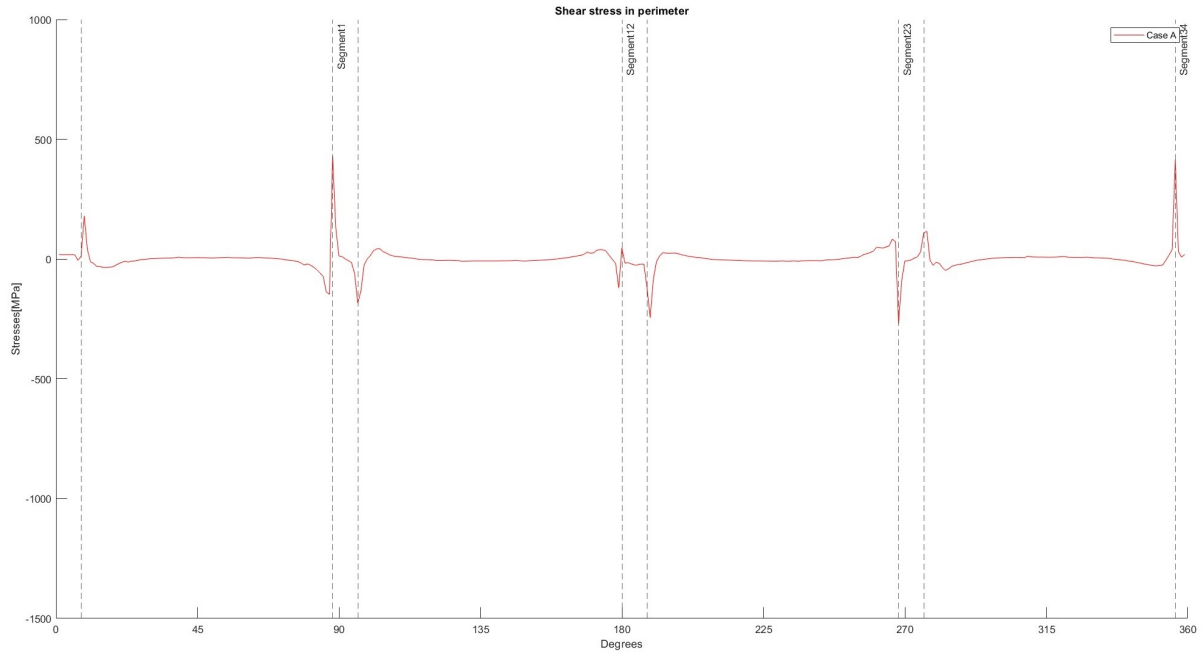

Figure 4.12: Shear stress in base of caisson-ΘZ direction-Case A

The results from the above figures showed the most important component of the equivalent stress in case A. Nevertheless, the division in the components do not end at this point. The normal stress in tangential direction can be analysed in the two main components, the axial and bending stress. Thus, in figures 4.13 and 4.14, the out-of-plane axial and bending stress in the base perimeter of the caisson are represented. As obvious from the figures, the most influence in the normal stress component has the bending stress. This is resulted from the fact that not only the out-of-plane bending stress owns the largest values, compared to axial stress, but also they follow the same distribution in the perimeter of the caisson and demonstrate the same peak stresses at the support edges, in terms of location and direction, as the normal stress component. The bending stress distribution in tangential direction or otherwise around Z-axis shows that there is a difference in the outer and inner area of the caisson's base perimeter. More specifically, in outside perimeter compression is developed whilst the inner perimeter is in tension. The bending stresses around vertical Z-axis are caused by the large radial deformations (Figure 4.6). Therefore, is realized that in order to reduce the bending stress component and consequently the equivalent stress, it is important to reduce the radial deflection.

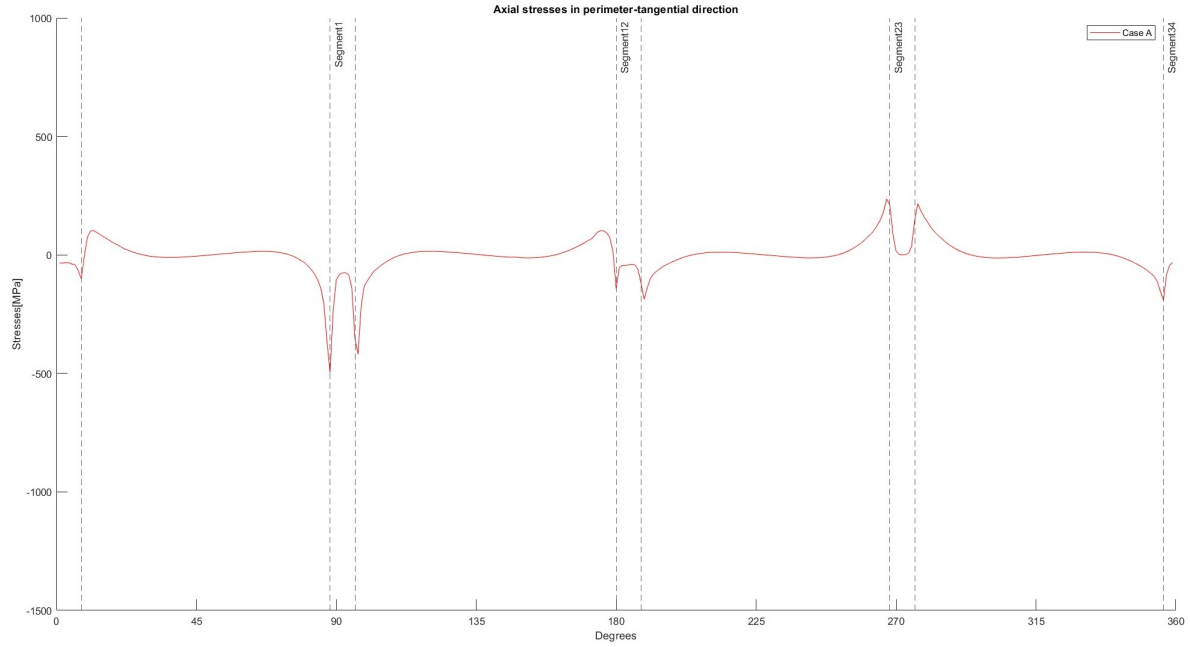

Figure 4.13: Axial stress in base of caisson-Case A

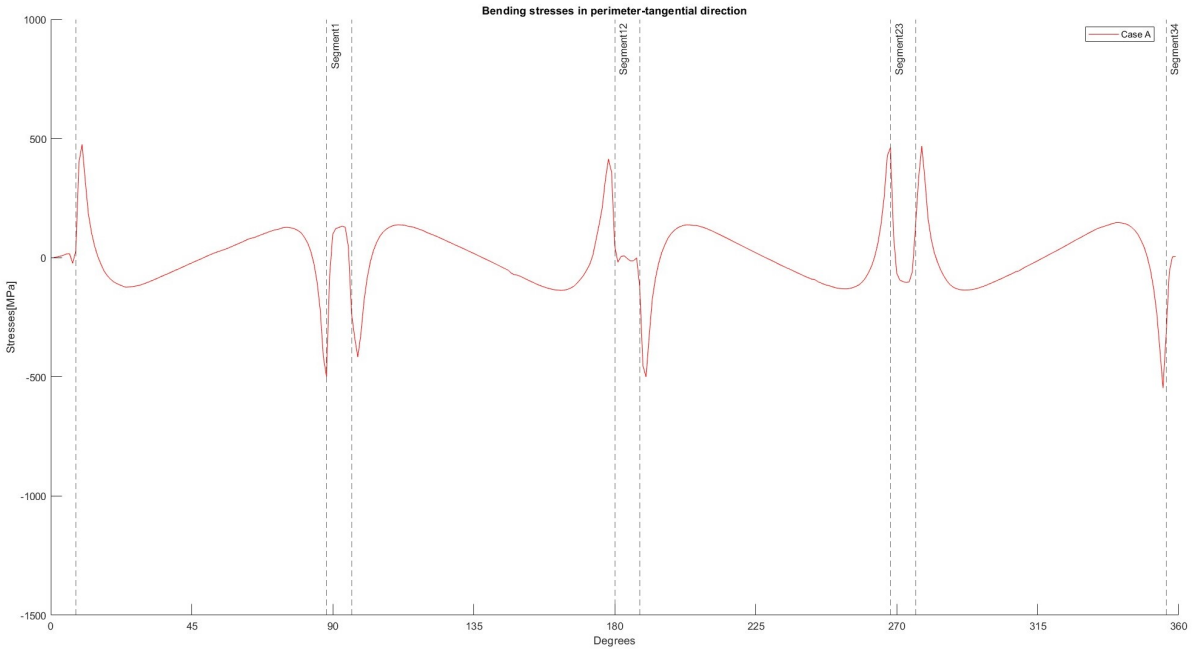

Figure 4.14: Bending stress in base of caisson-Case A

4.3. Parametric study

4.3.1. Directional deformations

Indeed, by focusing the study now on the parametric study (Cases A to D), there are several worth mentioning factors, which can be observed. Starting the analysis once more the deformations in every direction of the perimeter is examined, in order to understand the behavior of the supports, and hence of the barge, under this specific loading. The deformations are retrieved according to the cylindrical coordinate system of the system (Figure 4.1). Figure 4.15, illustrates the vertical deformations at the base perimeter of the caisson. In the figure, every deformation from cases A to D are represented, as well as the segments at which the supports are applied. As can be read from the image, Case A has the largest vertical deformation in the supports, while case C the minimum. Thus, the supported length influences the vertical deformation component. Vertical deformations exist in general in the supports, as the supports are simulated as distributed springs and follow both the grillage and the barge movement. Therefore, the more area is supported by elastic supports, the less the vertical deformations. Furthermore, the negative values point out that in every case the perimeter is in compression, due to the applied load and only a small part, area around the supported segment 23 is in tension.

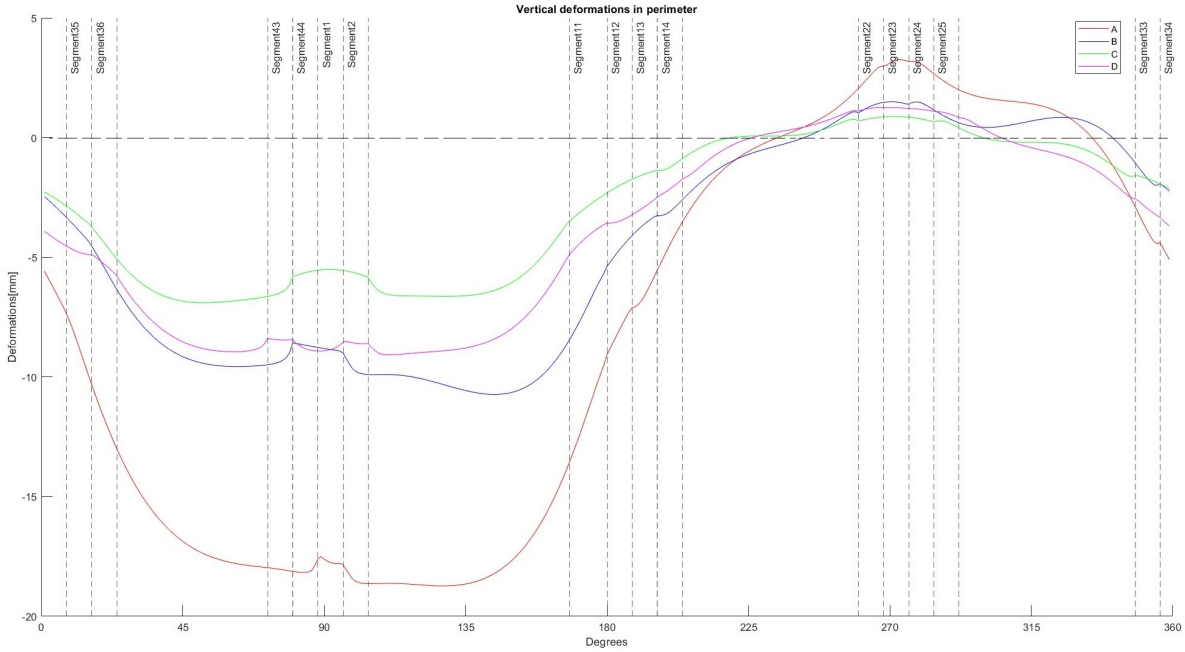

Figure 4.15: Vertical deformations in the perimeter

Continuing the study, figure 4.16 demonstrate the deformation in radial direction. Analyzing the image, it appears that the base perimeter tend to deform around the supports, similarly in every case, while in the supports the deformation is zero, indicating that the supports successfully restrain the movement in r-direction. Again the bigger deformations appear in Case A, while by increasing the length the deformations are reduced. The smallest deflections occur in Case D this time. In detail, observing the areas of the perimeter between two supports and focusing on two cases, A and B, two different conditions become apparent. From segments 1 to 12, where the same segments are supported, the deflections between the two cases are almost similar (in case B is a reduced by a little). On the other hand, from segments 12 to 23, where there is a 18% increase in the supported segments (additional 2 segments supported), the deflection is much more significant and amounts to 66% (20mm reduction).

Hence, this results in the fact that the more the unsupported area between the supports is reduced, the more the radial deformations are reduced as well.

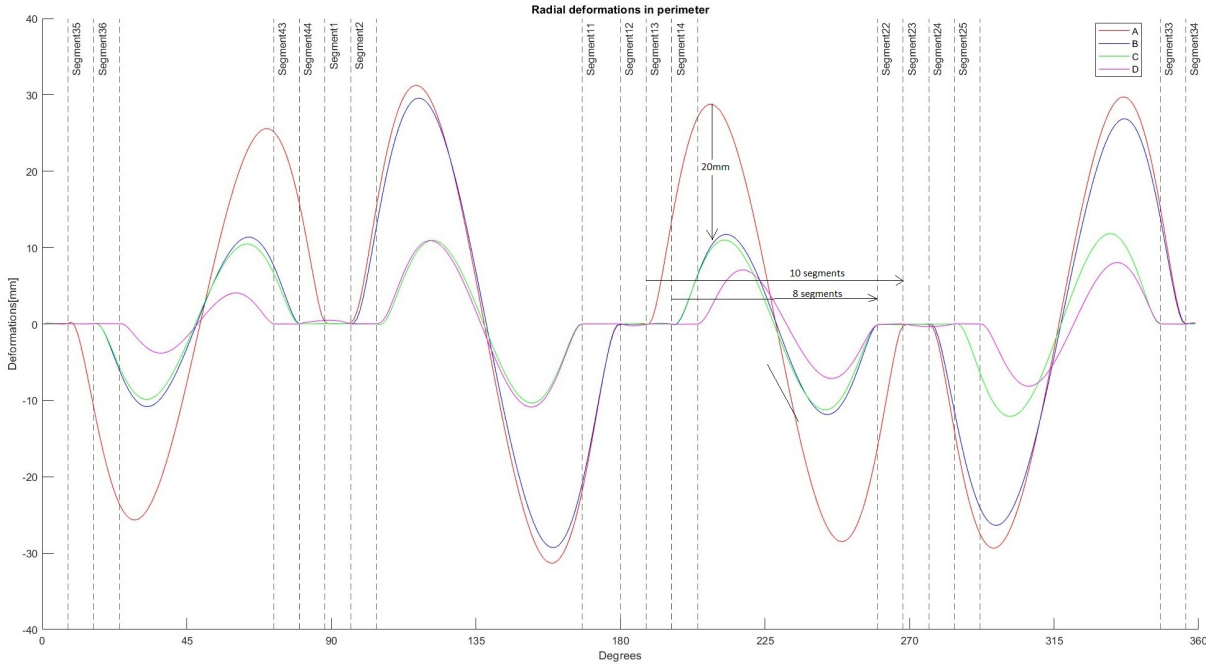

Figure 4.16: Radial deformations in the perimeter

In order to support that this interpretation of the result is not an isolated fact but it applies to a general extend, the following step in the evaluation of the results of tangential deformation. In figure 4.17, the tangential deformations of every support case are presented. Again, in the supported segments the deflection is zero, whilst in between the supports the perimeter tends to deform in and out of plane. Similarly to radial deformations, case D has the smallest deflection in tangential direction. By focusing now on the same areas between the segments but in cases B and C, the deflections seem to follow a similar trend. More specifically, in the area between segments 44 to 13, where there is 15% increase in the supported segments (additional 2 segments supported), the deflection in case C, appear to develop a 70% decrease in deflection (9mm reduction), whilst in segments 12 to 23, where same percentage of segments are supported, the deflection has an insignificant decrease (almost similar). Therefore, it is obvious that the influence of the unsupported area in the behavior of the caisson is much more significant than the length of supports.

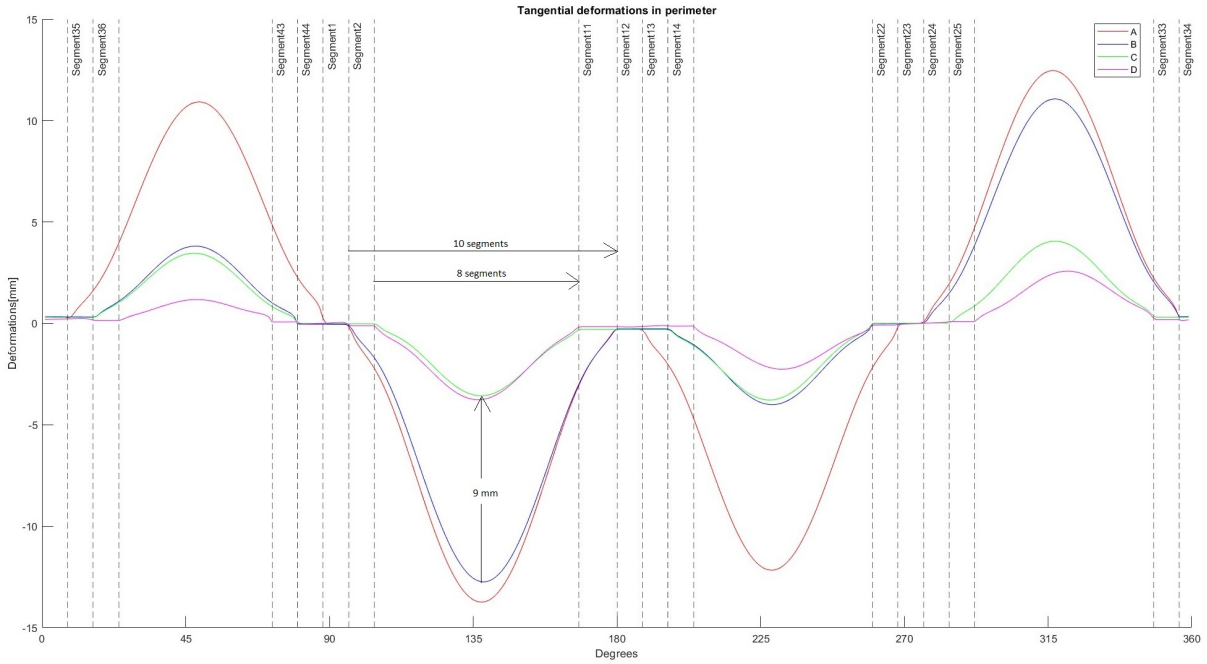

Figure 4.17: Tangential deformations in the perimeter

4.3.2. Equivalent von Mises stress in the perimeter

Now that is clear how the perimeter is distorted, it is time to observe as well what happens with the stresses that causes this behavior. To begin with the equivalent von Mises stress, in the perimeter of the caisson is demonstrated for every case in figure 4.18, as well as the main focus areas.

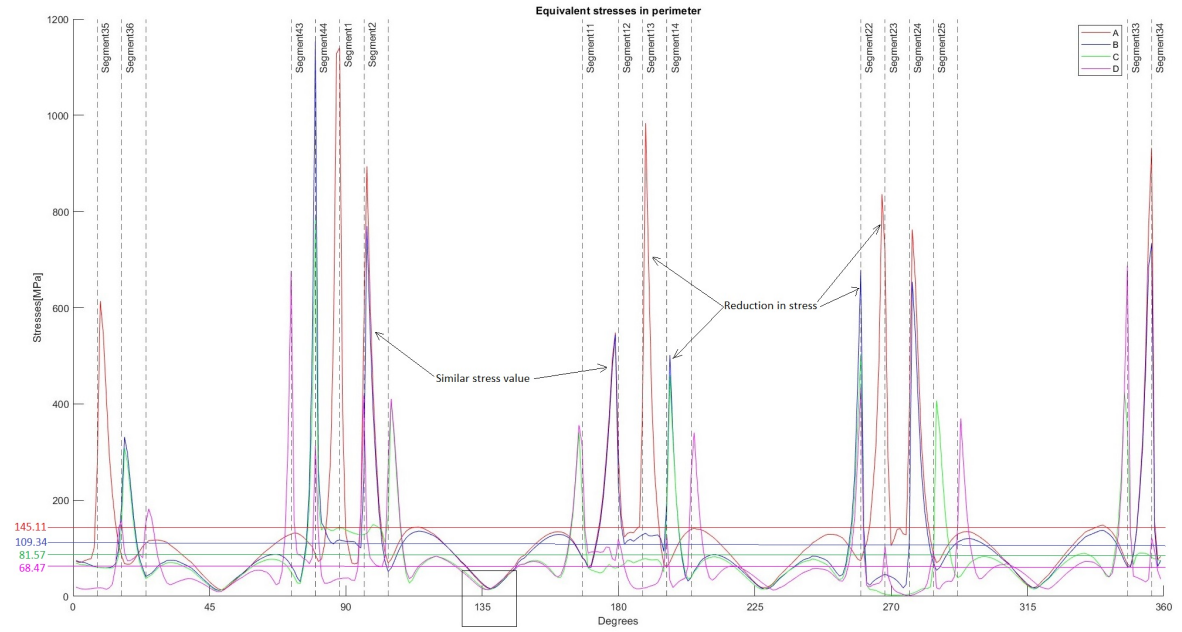

Figure 4.18: Equivalent von Mises stresses in perimeter

In figure 4.18, the equivalent stresses are presented for every case and for whole perimeter of the cais-

son. The segments where the supports exist for every case can also be seen in the image. As can be observed, the stresses show spikes at the edges of supported segments, while in the rest of the perimeter are evolving in a wave with an amplitude of 100 MPa, as appeared in the rest of the skirt (figure 4.2). This is reasonable as the force is transferred from the caisson to the barge through the edges of the grillage beams. Furthermore, the figure indicates the average values of stresses for each case (on the left), each of them being closer to the developed wave outside the supports rather than the high peaks which occur only locally. In every case, regardless the change of the parameter, it appears every time that the average stresses are reducing, with case D having the lowest values. What is also interesting is that in every case the stresses develop a peak in a different location, however they seem to reduce at the same value (close to 0) and almost at the same point in the perimeter. Thus, it becomes clear that regardless of the location or the length of the supports, the length of the perimeter is so large that the stresses would reduce significantly close to 0 at the same location. When examining the peaks, the figure illustrates that there can be differentiation between 2 cases. More specifically, examining for instance cases A and B, it is observed that between segments 1 and 12 where the same segments are supported, the stresses are almost similar. On the contrary, in between segments 12 and 23, where each support is increased by one segment, there is a great reduction. For further analysis, tables 4.1 and 4.2 were created.

Table 4.1: Reduction in stresses for every case- Segments 12 to 23

Segments 12-23	***Total number of segments: 11***				
Cases	**Unsupported segments**	**Unsupported area (%)**	**Decrease in stresses (%)**	**Decrease in stresses (%)**	**Decrease in stresses (%)**
A	9	81%	*base scenario*	-	-
B	8	73%	51%	*base scenario*	-
C	8	73%	55%	7%	*base scenario*
D	7	63%	70%	40%	34%

The above table analyses the reduction in peak stresses that appear in every case, in the unsupported area between the supported segments 12 and 23. For every case the unsupported area is defined in number of segments (column 2) and in percentage (column 3). In the rest columns, the decrease in stresses is indicated (in percentage), first from case A and subsequently from cases B and C. It can be observed that from cases A to B and C to D, where there is a decrease of the unsupported segments, even by 1, there is a significant decrease in stresses, 51% and 34% respectively. Opposed to that, from case B to C where the number of unsupported segments in this area remain the same, there is a inconsequential reduction of 7% , even though the number of supported segments in the whole perimeter has been doubled. Finally, it is important to mention that cases B and D, which they have the same number of segments supported in the whole perimeter, show a great difference in stresses (40%) in this area, only because the unsupported segments there, have been reduced by 1.

Table 4.2: Reduction in stresses for every case- Segments 44 to 13

Segments 44-13	***Total number of segments: 14***				
Cases	**Unsupported segments**	**Unsupported area (%)**	**Decrease in stresses (%)**	**Decrease in stresses (%)**	**Decrease in stresses (%)**
A	12	86%	*base scenario*	-	-
B	12	86%	9%	*base scenario*	-
C	8	57%	52%	47%	*base scenario*
D	8	57%	54%	49%	2%

In table 4.2, similarly to the previous table, the reduction in peak stresses can be seen in unsupported area between supported segments 44 and 13. At this table, it seems that between cases A and B and between C and D, the same number of unsupported segments exist. Based on the results of table 4.1, it is expected that comparing these cases, an insignificant reduction in stresses should

appear. Indeed, the table indicates that between cases A and B there is a 9% reduction and between C and D, a 2% reduction. On the contrary, comparing cases B to C (or D), where there is a reduction in unsupported area by 4 segments, the stresses are reduced by 47% (or 49%).

As aforementioned, the stresses appear minimum at the same location regardless the change in the boundary conditions. However, as seen in figure 4.18, the point where they start to dissolve changes in every case, thus implying that there is an influence of the supported segments in the development of the wave in the unsupported area. Delving into this issue, it is useful to measure the distance of the point where every stress starts to decrease, in the unsupported area, to the middle of the supported segment. For better understanding figure 4.19, shows the equivalent stress in the perimeter of case A. In the figure is indicated the desired measurement as influence zone, which extend from the amplitude of the wave (start of decadence) to the middle of the supported segment.

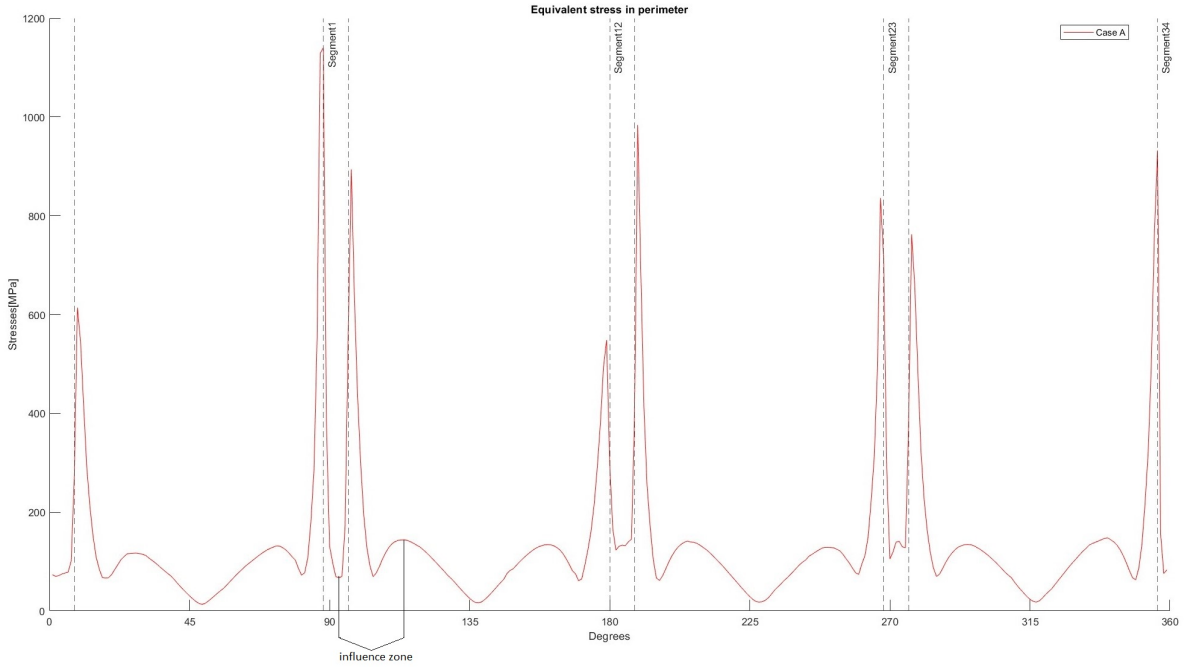

Figure 4.19: Equivalent von Mises stresses in perimeter-Case A

Based on figure 4.18, the influence zone was measured for every case. Thus, table 4.3 was created. The measurements were taken from the amplitude of wave in the unsupported area from segments 14 to 22, to the middle of the nearest support for every case, as also shown in figure 4.19. From the table can be observed that the influence zone changes every time when increasing the length of the support (Cases A to C) and not when the configuration has changed (Case D) and the unsupported area between two supports is decreased. Therefore, it is proven that the length of the supports influences indeed the point at which the stresses start to reduce. The longer the support, the more the influence zone is increased and thus, the further the stress start to deplete.

Table 4.3: Characteristic length for every case

Cases	Length of supports [m]	Supported segments	Influence zone [m]
A	0.698	S12	1.5
B	1.396	S12-S13	2
C	2.094	S11-S13	2.5
D	0.698	S14	1.5

It is noticeable that in the peaks, the values of the stresses are much higher than the material's yield limit (335 MPa). This indicates that the structure will enter the plastic region and experience permanent, plastic deformations. However, this occurs only in some elements on the perimeter area of the caisson, which might be minor compared to the caisson's high dimensions. In some cases, a small percentage of yielding is acceptable. According to EN-1993-1-5 2007, an acceptance criteria of 5% in principal strain is accepted. If the value of plastic strain caused by yielding is below 0.05 then the yielding is accepted and therefore the boundary conditions are adequate to support the load. However, in order to reach to a result a non linear analysis is required. Since at this study a linear analysis is performed after the stresses have reached the yield limit a redistribution of stresses is expected in the caisson. Further analysis will follow in the subsequent section about non linear analysis.

4.3.3. Stresses components in perimeter

Now that the equivalent stresses are assessed for every case, it is useful to retrieve as well it's significant components. As already examined in the previous section, it is conclude that the most dominant components are the normal stresses in tangential(Θ) and vertical(Z) direction and shear stress in ΘZ. The components are retrieved based on cylindrical coordinates system. By comparing the results, it was discovered that for every case the most important component turned out to be Normal stress in tangential direction, due to its largest values and the fact that the equivalent stresses follow the same pattern in their development in the perimeter. Subsequently, the normal stress in tangential direction was analysed in its two main components, axial and bending stress. Out of the comparison of them two it was concluded that the bending stress in Θ-direction has the most significant values and therefore the most influence in the normal and finally in the equivalent stress.

Thereafter, it will provide more insight to compare the trend of the bending stresses for every case. In figure 4.20, the development of out-of-plane bending stress in the perimeter is illustrated for every case. As obvious from the figure, the trend of bending stress is similar for every boundary condition case. However, the spikes in bending stress seem to vary in the same way and appear at the same locations as the ones in equivalent stress. For more explanation tables 4.4 and 4.5 were created.

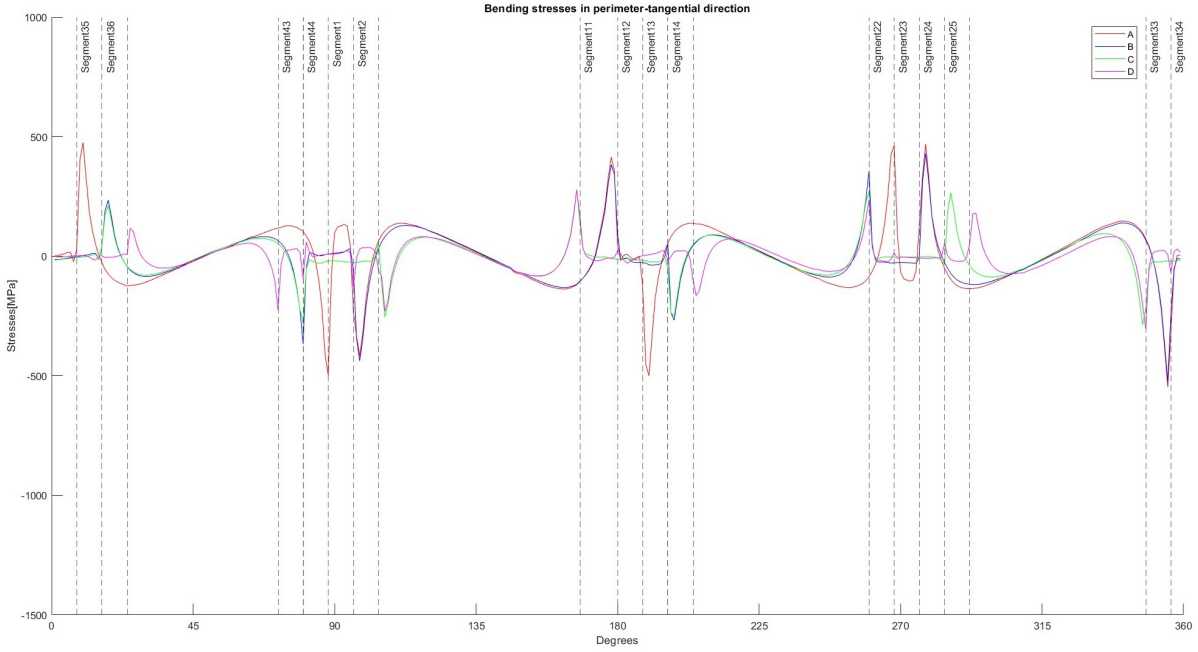

Figure 4.20: Bending stresses in perimeter

Table 4.4, demonstrate the decrease in the peaks of bending stresses for every case in the unsupported area between segments 12 and 23. It is observed that between cases A and B as well as in C and D, where there is a reduction of approximately 10% in the unsupported area for each comparison, the bending stresses decrease by 46% in the former and by 45% in the latter. Opposed to that in between cases B and C, where there is no change in the unsupported segments of this area, there is an insignificant 4% reduction of stresses. Thus, it is clear that the bending stress component behave similarly to the equivalent stress, when there is a change in the unsupported area between two supported segments.

Table 4.4: Reduction in bending stress for every case- Segments 12 to 23

Segments 12-23	***Total number of segments: 11***				
Cases	**Unsupported segments**	**Unsupported area (%)**	**Decrease in stress (%)**	**Decrease in stress (%)**	**Decrease in stress (%)**
A	9	81%	*base scenario*	-	-
B	8	73%	46%	*base scenario*	-
C	8	73%	49%	4%	*base scenario*
D	7	63%	67%	47%	45%

Respectively with the research in the equivalent stress, the unsupported area between supported segments 44 and 13 was investigated. Once again, between cases A and B, C and D, where there is no change in the unsupported segments, there is no decrease in the peaks of stresses. On the other hand, between cases B and C (or D), there is a 29% reduction of the unsupported area and that corresponds to a 39% decrease in the bending stress peak. Likewise, table 4.2, the bending stresses follow similar and even less distinct changes between the peak values and always influenced by the unsupported area.

Table 4.5: Reduction in bending stress for every case- Segments 44 to 13

Segments 44-13	***Total number of segments: 14***				
Cases	**Unsupported segments**	**Unsupported area (%)**	**Decrease in stress (%)**	**Decrease in stress (%)**	**Decrease in stress (%)**
A	12	86%	*base scenario*	-	-
B	12	86%	0%	*base scenario*	-
C	8	57%	39%	39%	*base scenario*
D	8	57%	39%	39%	0%

4.3.4. Buckling

Buckling is a structural failure condition, which occurs in structures mostly under large compression load, suddenly and is characterized by large deflections, perpendicular to the axis of the column. Usually, structures under compression may buckle, when the applied load reaches the critical buckling load. In order to evaluate critical buckling (bifurcation) load of structures, usually eigenvalue buckling analysis is used for this estimation. The analysis is a linear perturbation procedure (E. Ellobody 2014), which calculates buckling load magnitudes that cause buckling and the associated buckling modes. Eigenvalue buckling can be used after the structure is pre-loaded. During this process, the load multipliers (eigenvalues) and buckling mode shapes (eigenvectors) are predicted. An incremental loading pattern is defined in the eigenvalue buckling prediction step and its magnitude is scaled by the load multipliers. The critical buckling loads are then equal to the preloads plus the scaled incremental load. The buckling mode shapes are normalized vectors and do not represent actual magnitudes of deformation at critical load. The most important result out of the analysis is usually the buckling mode shapes, since they predict likely failure modes of the structure. Normally, the lowest (positive) load multiplier and buckling mode are of interest, mainly because higher buckling modes have no chance to take place.

In order to check if the applied load will be responsible for buckling an eigenvalue buckling analysis was performed for every case in Ansys. In order to ensure that enough modes will be extracted for buckling evaluation, in total ten (10) modes were found. In table 4.6, the eigenvalues for every buckling mode of case A can be observed. As can be seen, the first two eigenvalues are negative, which indicate that the structure would buckle if the load was on the opposite direction. Generally, the load multiplier is an indicator of the factor of safety against buckling or the ratio of the buckling loads to the currently applied loads. In order to evaluate if buckling is possible to occur mode 3, which is the lowest positive value load multiplier and mode was chosen.

Table 4.6: Load multipliers in every buckling mode for every case

	Cases			
Modes	**A**	**B**	**C**	**D**
1	-5.4692	-6.2763	-6.2832	-6.2859
2	-4.7515	-5.4628	-5.4742	-5.4648
3	3.1053	-4.7029	-4.7233	-4.7228
4	5.0174	4.9995	5.0122	5.0097
5	5.4205	5.4067	5.413	5.4168
6	5.4303	5.4299	5.4232	5.4245
7	5.4929	5.4984	5.4906	5.4833
8	5.9935	6.0015	5.9951	5.9993
9	6.087	6.094	6.0824	6.087
10	6.1676	6.1711	6.1653	6.1569

In general, a high factor or a high load factor of safety against buckling is above 3 (Akin 2010). As can be seen the load multiplier has a value of 3.8137, which at a first level is considered safe. However, in order to support this argument, figure 4.21 is utilized. According to this, since BLF is above 1, buckling is not potential to occur at this load. The critical estimated load that buckling supervenes is above the applied load at this case.

BLF Value	Buckling Status	Remarks
>1	Buckling not predicted	The applied loads are less than the estimated critical loads.
= 1	Buckling predicted	The applied loads are exactly equal to the critical loads. Buckling is expected.
< 1	Buckling predicted	The applied loads exceed the estimated critical loads. Buckling will occur.
-1 < BLF < 0	Bucklin possible	Buckling is predicted if you reverse the load directions.
-1	Buckling possible	Buckling is expected if you reverse the load directions.
< -1	Buckling not predicted	The applied loads are less than the estimated critical loads, even if you reverse their directions.

Figure 4.21: Buckling load factor (BLF) evaluation (Akin 2010).

After applying eigenvalue buckling in the other cases as well, it was concluded that once more in every case. For cases B to D, mode 4 was the one the lowest positive eigenvalue. However, as seen in table 4.6, again in each there is no significant cause for concern about buckling in the caisson, under this specific combination of loads. In Figure 4.22, can also be observed the figures derived from Ansys, where they indicate also the places where buckling will occur for the specific modes explained above. As illustrated in every case buckling is not possible in supports. Nevertheless, in case A buckling in mode 3 will occur in the skirt, whilst in the rest cases buckling takes place in the stiffeners. This is reasonable, since in case A, all the load is taken by the four(4) supports or segments and therefore increasing the possibility of buckling in the skirt. On the contrary, the more area of the perimeter is supported, the more the skirt is not in danger to buckle.

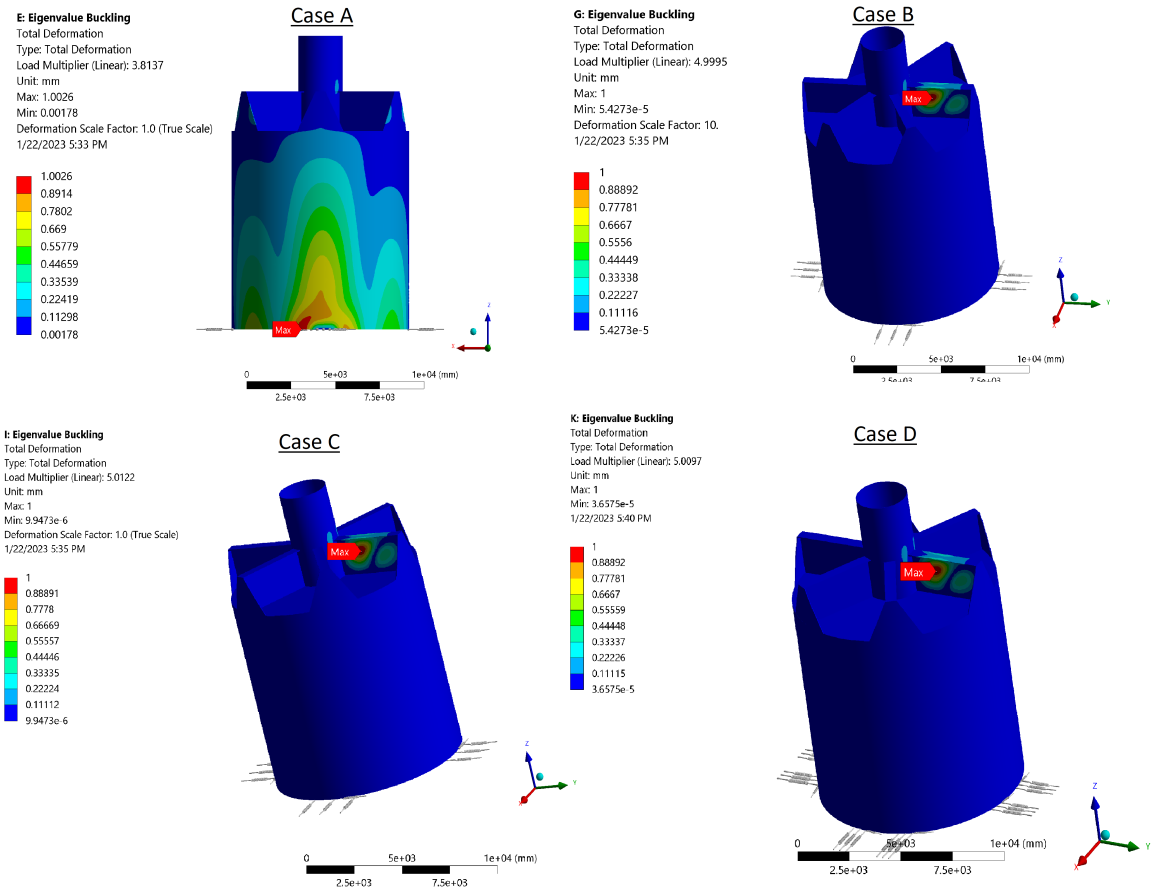

Figure 4.22: Buckling for every case

At this point it is made clear that in case A only mode 3 reveals that buckling may occur in the skirt, whilst the rest of the modes show buckling possibility either on the lid or the stiffeners. On the other hand, for the ten (10) modes investigated in cases B to D, buckling is only possible on lid or stiffeners. In order to investigate buckling effect in the skirt even further, the modes for the analysis where increased so that to discover at which buckling mode and hence buckling load factor, might buckling occur in the skirt for cases B to D. Analytically, sixty (60) modes were retrieved for the analysis. In table 4.7, the results from the analysis can be observed. The table shows that for every case buckling in the skirt occurs for a different mode and corresponding buckling factor. Once more, the applied load is not of a high risk to cause buckling in skirt, as it has to be increased by a higher load factor in every case B to D, in order to reach the buckling load. Furthermore, as seen on the table, the load factor is increased every time from case A to C, whilst in case D is almost equal to case B. Since cases B and D, have the same number of segments supported (different configurations), it can be realised that the length of the supports influences buckling mode. More specifically, by increasing the length of the supports the load factor is also increased, signifying that the working loads endure even more the structure's buckling capacity.

Table 4.7: Buckling modes and load factors in the skirt of the caisson

Cases	Buckling mode	Buckling load factor
Case A	mode 3	3.11
Case B	mode 25	7.43
Case C	mode 54	12.14
Case D	mode 29	7.79

Nevertheless, it is important to observe as well the location in which buckling takes place. Figure 4.23 illustrates the buckling shape in the skirt for every case which has been studied. For every case, buckling is developed in the part of the skirt which experiences the most compression and where the highest stresses exist. Evidently, the shape of buckling is similar every time except of the maximum buckling points which differs.

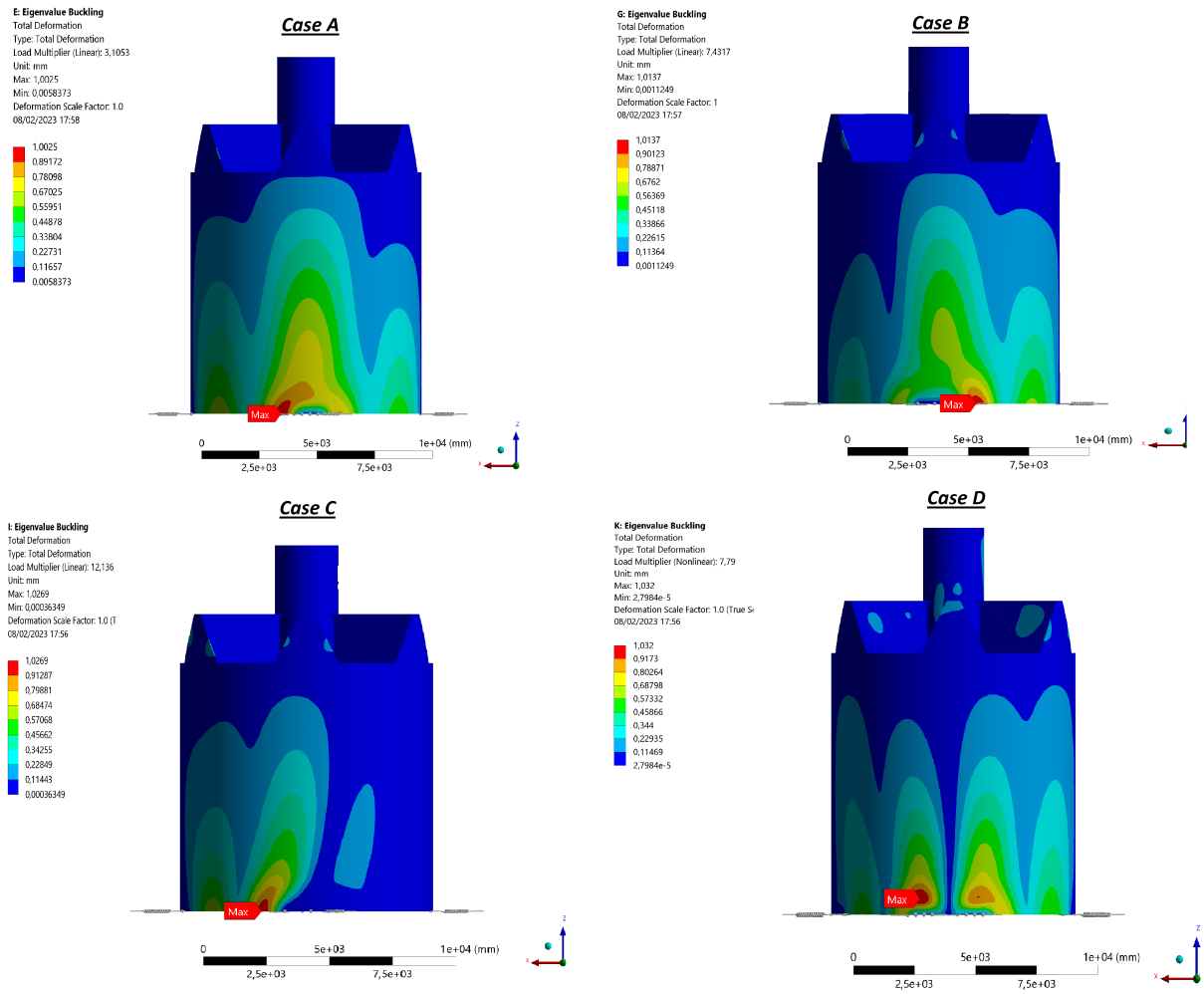

Figure 4.23: Buckling in skirt for every case

4.4. Sensitivity study

Since the cases A to D have been studied and compared to each other, it is time to examine what are the results when the stiffness in the supports has changed. For this reason cases E and F where created, where the stiffness in two of the supports has been replaced to fix supports (Table 3.3). These cases have been compared to case A, as can be seen in the following figures. In figure 4.24, the vertical deformations are illustrated. It appears that the largest deformations are in segment 1 in case A, while in segment 23, they appear on case F. In any case though the smallest vertical displacements appear on case E. This indicates that when two(2) out of four(4)of the supports are infinite stiff then the vertical deformations are reduced. Especially, when the fix supports are located in the same direction as the direction of the moment (case E), and Mx is received by both of the supports, then the vertical deflection in every support is limited compared to case F, where the fix supports are applied in the neutral axis of the moment.

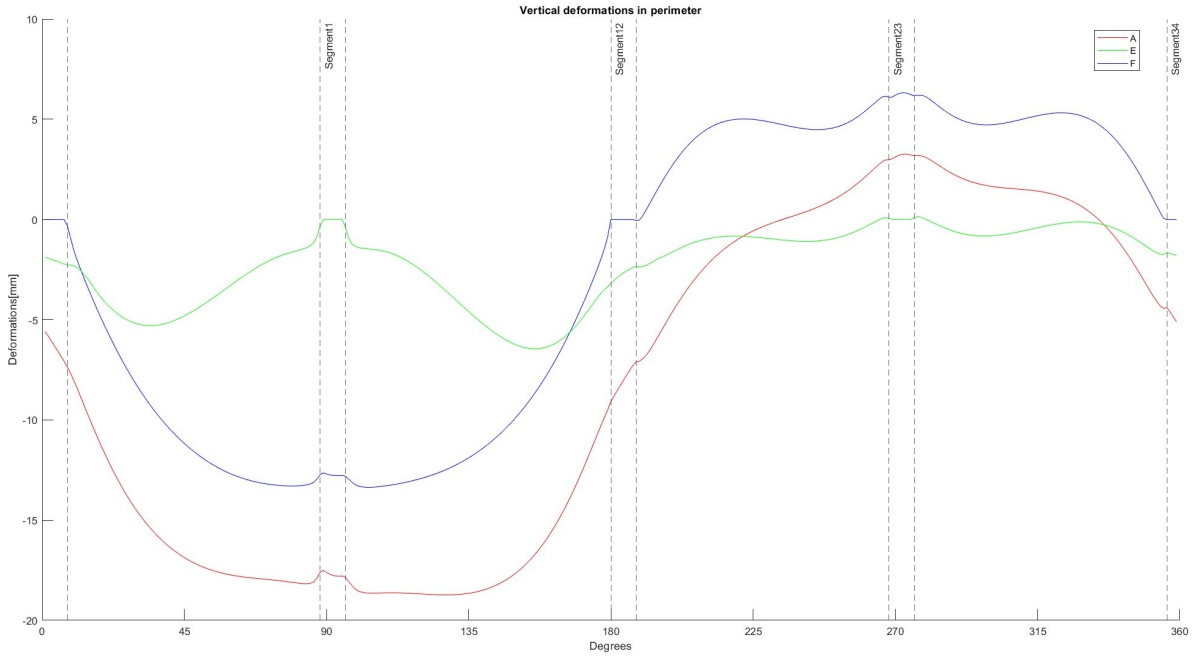

Figure 4.24: Vertical deformations in the perimeter

As far as the tangential and radial deformations in the support is concerned, the same result may be concluded. Figures 4.25 and 4.26, illustrate that in both cases, from segments 34 to 12, case E has the largest deflection and case F the smallest, while in the rest area the deflections are reversed. Both figures also show that the vertical elastic support stiffness affects the radial and tangential deformations in the caisson and therefore also the stresses. Furthermore, by comparing the amplitude of the waves between the cases, it is realized that between cases E and F, exchange the amplitudes of their waves in the unsupported areas of the segments. More specifically, by observing the area from 0 to 180 degrees and case F, the value of the amplitude of the wave is similar to that of case E, in the area from 180 to 360 degrees. Finally the conclusion is reached that when comparing cases E or F to case A, it appears that there is a redistribution in deflections rather than a reduction for example when the fix supports are applied.

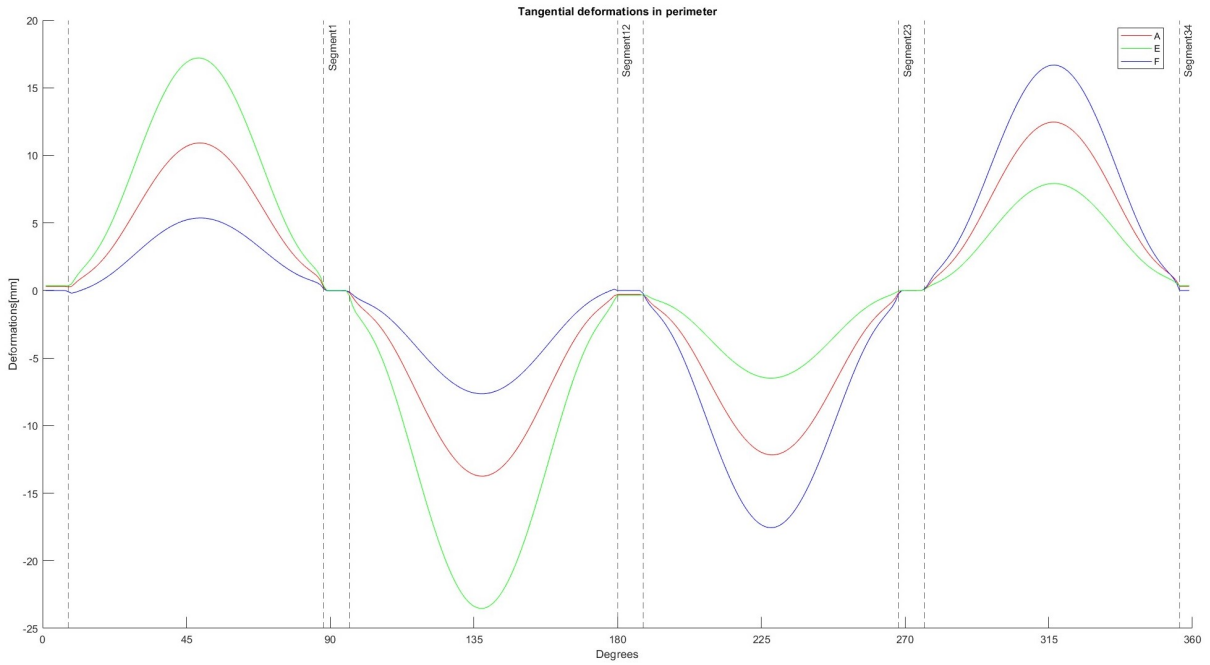

Figure 4.25: Tangential deformations in perimeter

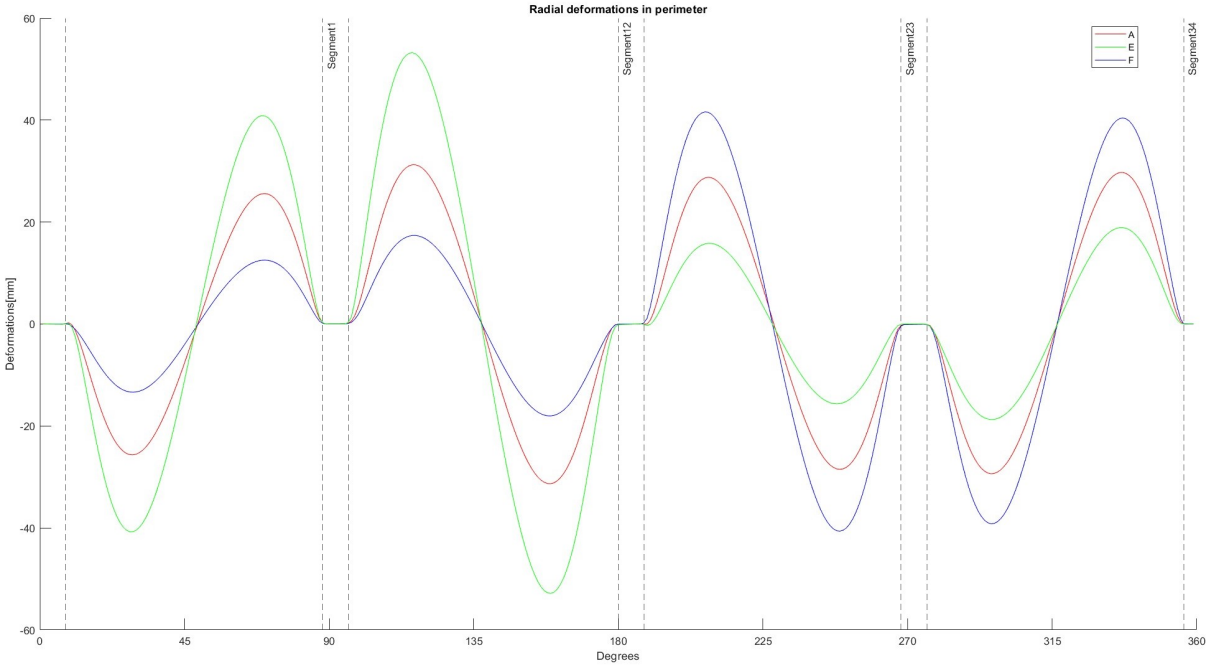

Figure 4.26: Radial deformations in perimeter

Now that the behavior of the perimeter in the three cases has been established, it is useful to observe as well the equivalent von Mises stresses in the perimeter, so that a conclusion might be reached. In figure 4.27, the equivalent stress in the perimeter is illustrated for cases A, E and F. As can be seen, the same change existing in directional deformations, applies also here. From 0 to 180 degrees, the peak stresses in case E are much higher than case A, while in the rest of the area are lower. At the

same area, the peaks in stresses in case F, are much lower than case A. It is reminded that from 0 to 180 degrees, the radial and tangential deformations for case E, were much higher as well. On the other hand, from 180 to 360 degrees, peak stresses in case F is much higher than case A and case F is lower than those in case A. Once more similar behavior in each case can be seen in the directional deformations as well (Figures 4.26 and 4.25). Therefore, in cases E and F, where a combination of fix and elastic support is applied, there is no reduction in stresses or deflection, but rather a redistribution. It is realized that when stiffness is reduced there is no significant change in the results. Thus, it may be concluded that the reduction in stiffness as a parameter is not as beneficial in the support of the caisson, compared to the other cases (B to D), where the length of the supports or the configuration is changed.

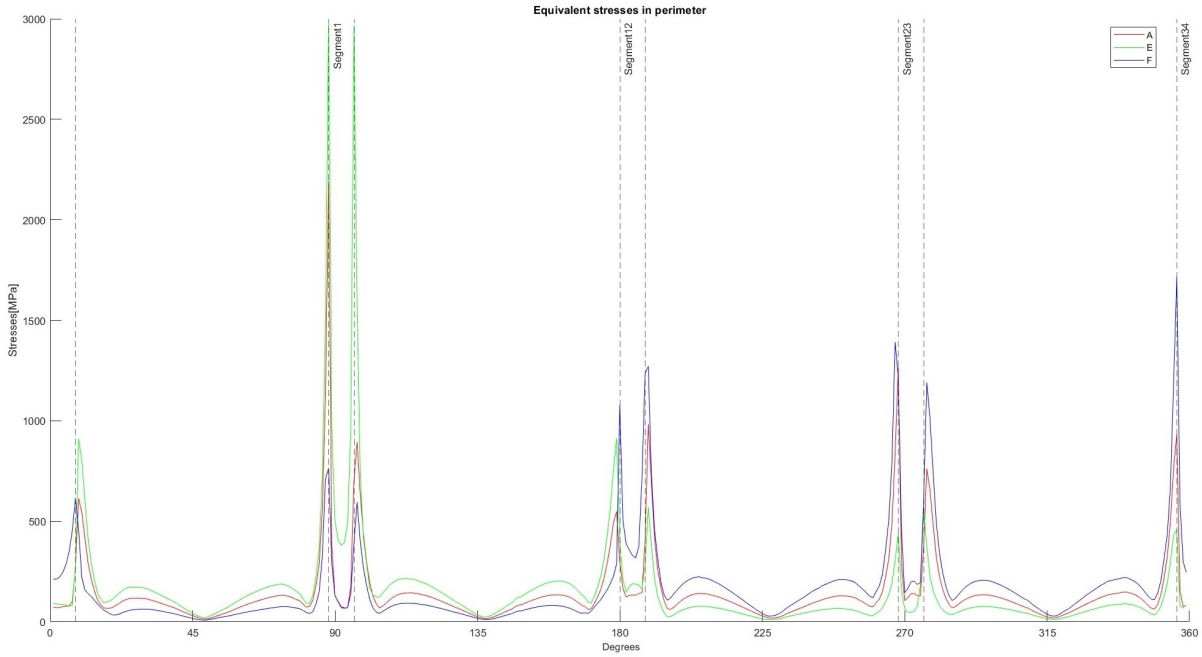

Figure 4.27: Equivalent stress in perimeter

4.5. Non-linear material behavior

As stated in the previous results, the very high peaks appeared in stresses (Figure 4.18) are much higher than the factored yield limit of the material (309 MPa). This indicates that the structure will enter the plastic region and experience permanent, plastic deformations. According to DNVGL-OS-C102 2020, local peak stress may be accepted for small local areas, provided satisfactory redistribution of stresses to the adjacent structure is possible. Therefore, is important to identify whether the high stresses and yielding of the material is acceptable. For this reason a non-linear analysis should be performed. The non-linear analysis was applied in every case of the parametric study, in order to develop a better insight in the results of the linear analysis.

In order to apply the non-linear analysis, the model should change some of it's material properties from the beginning of the analysis. Non-linear modeling in Ansys requires a plasticity model to be chosen and the stress-strain curve to be included in the material properties. There are many options in Ansys to chose from in order to apply plasticity in the system. At this case multilinear isotropic hardening model was chosen, defined by a series of plastic stress-strain points. This model requires certain parameters as inputs in order to model the material. The material should be modeled as a combination of a stepwise linear and power law with a yield plateau, given in true stress-strain parameters (DNVGL-RP-C208 2019). For inserting the inputs, the guidelines from DNVGL-RP-C208 2019 is followed. More specifically, the stress-strain curve is recreated as appears in figure 4.28, by making use of the values for the material parameters for S355 (Table 4-4) and the following equation:

$$\sigma = K(\epsilon_p + (\frac{\sigma_{yield2}}{K})^{\frac{1}{n}} - \epsilon_{p_y 2})^n \quad \text{for} \quad \epsilon_p > \epsilon_{p_y 2}$$

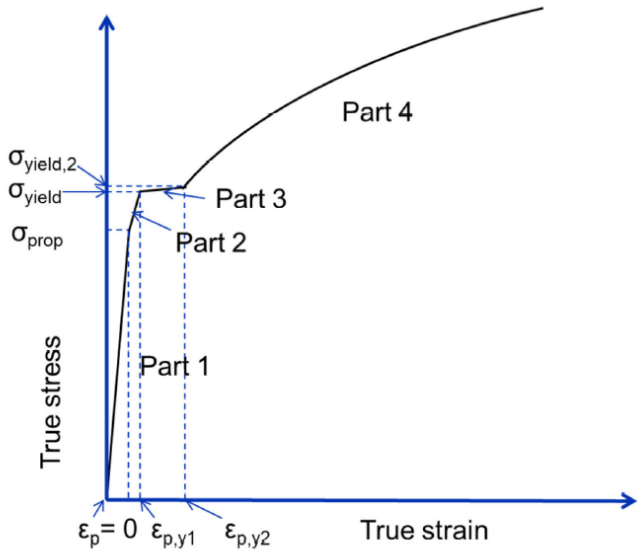

Figure 4.28: Definition of stress-strain curve (DNVGL-RP-C208 2019).

With the implementation of stress and strain curve in the properties of the material, the non-linear behavior of the material is now included. Furthermore, for the correct application of safety factors in the non-linear analysis, the applied loads are multiplied with the material factor (1.15), since the required yield limit in the analysis is now set at 335 MPa. Therefore, the applied load for the non linear analysis are presented in table 4.8.

Table 4.8: Applied loads in non linear analysis

Forces			**Accelerations**	
Fz [KN]	Fy [KN]	Mx [KNm]	az [m/s^2]	ay [m/s^2]
Heave	*Sway*	*Roll*	*Heave*	*Sway*
-28750	6900	13800	14	-8

In order to evaluate the results, the plastic strain in every case should be retrieved. Table 4.9 indicates the maximum values of plastic strains in the skirt of the caisson. In every model the maximum value appears in supported segments, which are located every time, in y-direction of the global coordinates. In accordance to DNVGL-RP-C208 2019, the limit of the maximum allowable plastic strain is 5%. Comparing this to the values retrieved for every case it can be concluded that case A with plastic strain 7.4% exceeds the allowable limit, whereas cases B to D develops plastic strain with a value, way below the accepted limit. From the results is made clear that case C has the least plastic strain and therefore is realized that the more area is supported, the more the value of plastic strain is reduced.

Table 4.9: Maximum plastic strain in skirt of the caisson

Models	**Plastic strain [mm/mm]**	**Segments**
Case A	0.074	Segment 1
Case B	0.008	Segments 1-44
Case C	0.003	Segments 2-1-44
Case D	0.004	Segment 2

However, apart from the value of the plastic strain, the area in which plasticity occurs should also be evaluated. From the results in Ansys it appears that plasticity takes place in a small area in supported segments as shown in figures 4.29 to 4.32. It is important to remind that the meshing size influences the values of the results. However, since in case A the value of plastic strain is above the allowable limit, further analysis may be performed in this scenario.

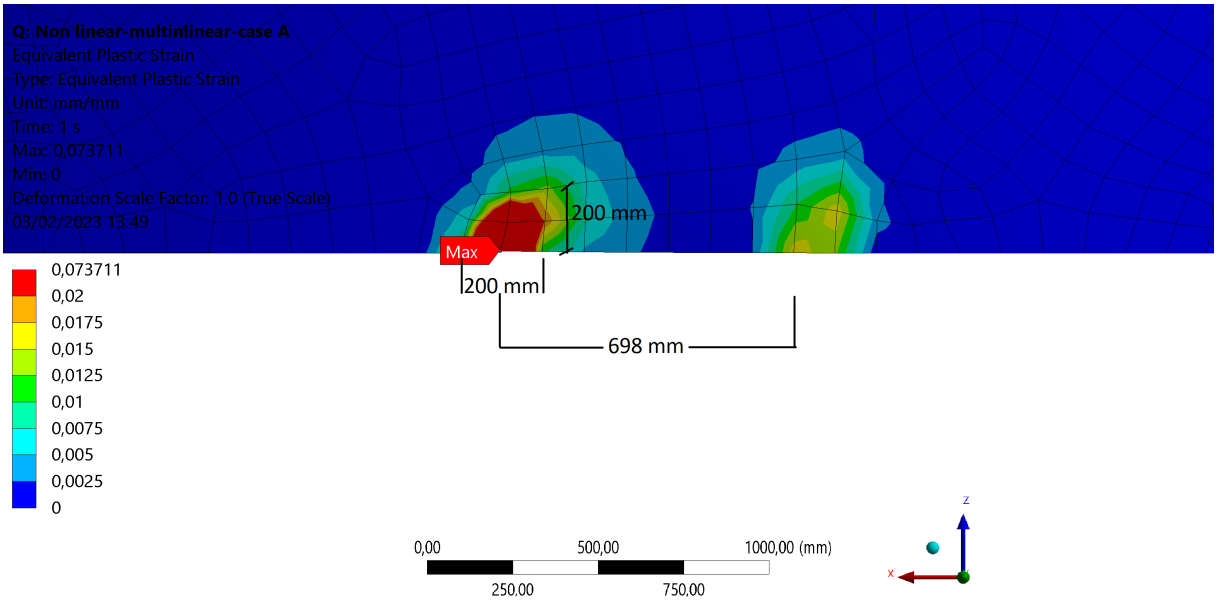

Figure 4.29: Area subjected to plastic strain-Case A

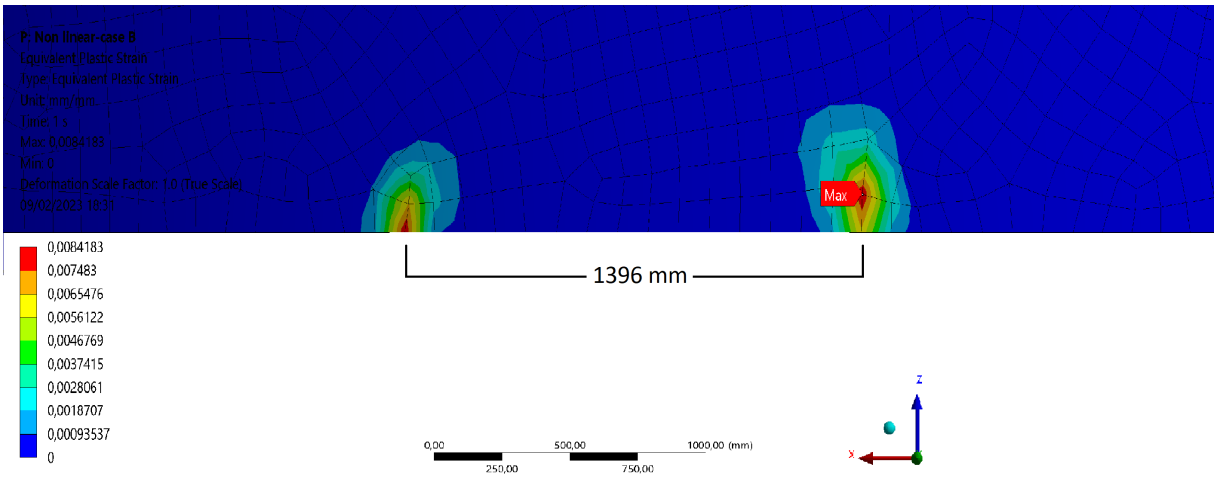

Figure 4.30: Area subjected to plastic strain-Case B

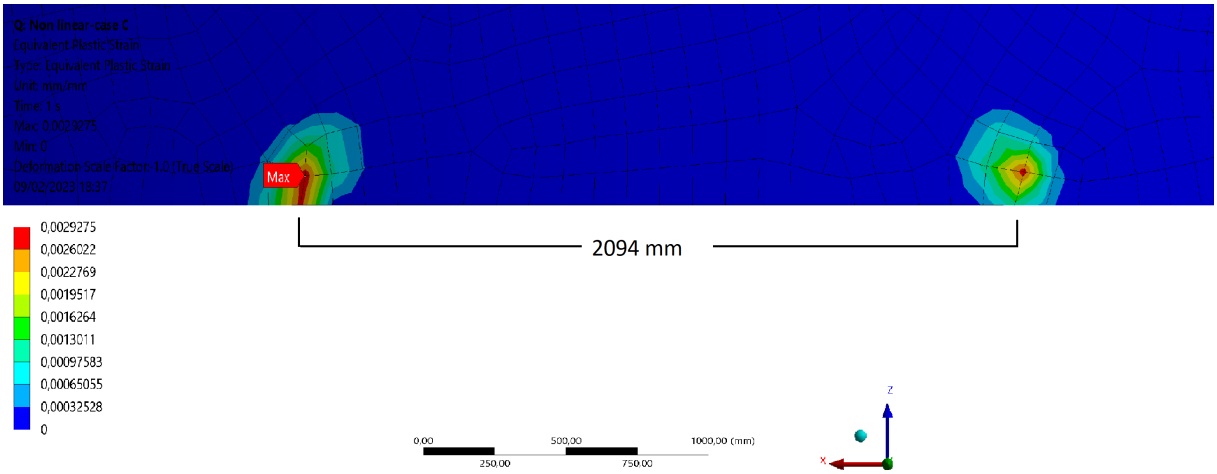

Figure 4.31: Area subjected to plastic strain-Case C

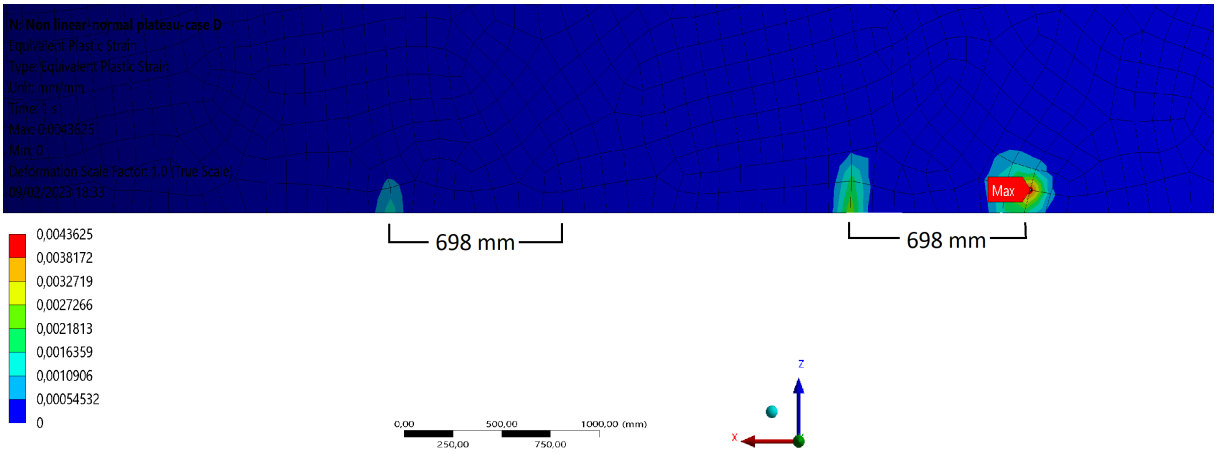

Figure 4.32: Area subjected to plastic strain-Case D

The sufficient check for case A, was performed under the requirements set in DNVGL-RP-C208 2019 for gross and local yielding. The structure should be checked for a general requirement for all areas subjected to plastic strains called gross yielding. With gross yielding is meant that plastic deformations with strain above 2% are taking place over a zone lyz > 20t in the direction of the maximum plastic strain (DNVGL-RP-C208 2019). By considering model 1, the measurements in Ansys show that four(4) elements appear with strain over 0.02. In the area where plastic strain exists, the element size is 100×100 and t =50mm as shown in figure 4.33. Therefore, by examining this element:

$$lyz = 4 \cdot 100 = 400 < 20 \cdot t = 1000$$

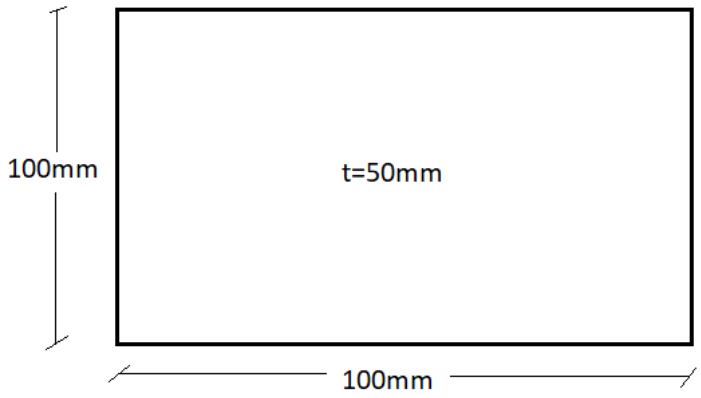

Figure 4.33: Element size in area subjected to plastic strain

Thus, gross yielding does not occur in the elements within the yielding zone. Yielding takes place in a limiting area. It will be due either to strain gradients or out of plane bending or a combination of these two effects. In figure 4.29 the strain distribution for case A, in support A (segment 1) is shown and the critical area of plastic strain is indicated. As can be observed although plastic strain is developed in most of the support's length, the critical area of plastic strain is located at the edge of the segment, in a very small zone. In detail, critical plastic strain zone, exceeding the value of 0.02, occupies almost 10% of the segment's area and nearly 0.5% of the supported perimeter. Consequently, local yielding check should take place within the yielding zone. Since plastic zone is defined as less than 20t, the maximum principal strain should be under the following constraint:

$$\epsilon_{crl} \leq \epsilon_{crg}(1 + \frac{5t}{3l})$$

,where

ϵ_{crg} = gross yielding critical strain
t = element thickness
l = element length in the direction of the maximum principal strain

Gross yielding principal strain is derived when considering the parameters from table 5-1 and figure 5-1 (DNVGL-RP-C208 2019), where calibration case CC01 is analysed:

$$\epsilon_{crg} = \frac{\delta_x}{l_0} = \frac{21}{450} = 0.046\ mm/mm$$

Therefore by performing the necessary calculations for the local yielding check:

$$\epsilon_{crl} \leq \epsilon_{crg}(1 + \frac{5t}{3l}) \Rightarrow$$
$$0.074 \leq 0.046(1 + \frac{5 \cdot 50}{3 \cdot 100}) \Rightarrow$$
$$0.074 \leq 0.084$$

Thus, the limitation for local yielding check applied in case A shows that the larger strains, taking place in the support is indeed within the limit for local yielding check and therefore considered acceptable. Non linear analysis for cases B to D, revealed that their estimated strain value is within the limit of the maximum strain value as stated by DNVGL-RP-C208 2019, and hence this concludes that the local peak stresses, which appear in the supports are acceptable and indeed lead in redistribution of stresses. Although, at the end every support cases have adequate structural capacity to support the caisson, the most beneficial support case should be determined in addition to the previous results. Considering all of the previously described results, case D comes across as much more optimal, with a maximum strain value much lower than the limit, so as not to add risk of yielding to the caisson and consequently allowing the development of peak stresses in the supports.

5
Conclusions and Recommendations

5.1. Conclusions

In this research, several aspects of the behavior of suction jacket caissons were analysed during their transportation. The study at a first stage was linear and parametric, by changing the boundary supporting conditions for every analysis. In total six conditions were examined and compared to each other, four in parametric study and two were analysed as a sensitivity analysis for the stiffness of the barge. The change of the supports, was distinguished between the change of the supporting length and the change of the configuration of supports, by distributing them in the available area. At a second stage the analysis was converted into non-linear for every case of the parametric study. For the evaluation of the behavior of the caisson at every boundary condition case, the results of the equivalent von Mises stress and its components were retrieved, as well as the deflection and buckling of the caisson was assessed. Thus, the conclusions of the study are summarized below:

- Across the skirt, the equivalent von Mises stresses are distributed evenly as a wave and at the bottom, where the supported segments are located, they show really high spikes, indicating that the supporting conditions of the thin walled caisson is something interesting to be investigated (Figure 4.2).

- Vertical deformations and the length of the supports are inextricably linked. Figure 4.15 shows that the more area is supported by distributed springs, the more the vertical deformations are reduced.

- Radial and tangential deformations indicate that there is an influence of the unsupported area between two supported segments and the deflection (Figures 4.17 and 4.16). When unsupported area between two supports is reduced the radial and tangential deformations per case are also reduced.

- Radial and tangential deformations also point out that the increase in the length of the supported segments have little to no influence in the amplitude of the deflections, when the supported segments in the different cases have the same distance with each other.

- Equivalent stresses demonstrate a general uniform development of wave in the perimeter with the exception of the edges of the supported segments, where very high spikes appear (Figure 4.18). The values of these spikes indicate that yield limit of the material is exceeded.

- Regardless of the case of boundary conditions, equivalent stresses obtain a minimum value always at the same location outside the supports, which denote that the length of the caisson's perimeter is so large that the distribution of stress is not influenced by the boundary conditions (Figure 4.18).

- Equivalent stresses in the perimeter show the same behavior as the deformation. More specifically, comparing cases where the supports have the same distance between them, the stresses demonstrate an insignificant change. However, once more when the unsupported area between two supports is reduced then the peaks in the equivalent stresses show a great reduction as well (Figure 4.18).

- The influence zone or the point at which the stresses start to decrease, in the unsupported area, is affected by the length of the supports. The longer the supports, the more further away the amplitude of stresses in the unsupported area begin to reduce (Table 4.3).

- The more important component of the equivalent stress is the bending stress component in tangential(θ) direction. Therefore, if this is limited, the high spikes in the equivalent stresses will be reduced as well (Figure 4.14).

- Similarly to the previous results, the out-of-plane bending stress component shows great reduction when the unsupported area between two supported segments is reduced (Figure 4.20).

- Increasing the stiffness in half of the supports will not cause any reduction in the equivalent stress component or in deformations. It is shown that probably this will lead to a redistribution of stresses in the supported perimeter, whilst maintaining the large peaks in stresses at the edges of the supported segments.

- The location of buckling differs for every case. In case A, mode 3 is the first possible buckling mode for the applied load, whilst for cases B to D, mode 4 is the first possible buckling mode. For case A, mode 3 shows that buckling will take place in the skirt, whilst for cases B to D, mode 4 shows that for each case buckling will occur on the stiffeners (Figure 4.22).

- For cases B to D, buckling in the skirt is more improbable to occur. When increasing the derived modes, it is discovered that buckling load factor is incremented for cases B,C and D (Table 4.7).

- The length of the supports, influences the buckling modes. When the length of the support is increased, the buckling load factor is also increased and therefore the applied loads subceed even mode the structure's buckling capacity (Table 4.7).

- Based on the non-linear analysis for case A of parametric study, the conclusion is reached that plastic strain is above allowable limit of 5%, however is still acceptable, since it meets the standards for local yielding check.

- The non-linear analysis for case D of parametric study, results in the fact that plastic strain is very small, bellow the maximum allowable limit of 5% and thus local peak stresses are acceptable providing a redistribution of stresses in the structure.

All the analysis was carried out with a purpose to answer the research questions raised in the introduction chapter. More specifically, the results fielded the answer to the first question about the optimal grillage design. As observed, out of all the cases which were analysed, the most beneficial grillage design corresponds to case D. In this support case, the results in stresses and directional deformations are the most promising, suggesting that the grillage design should be focused more on the reduction of the distance in between the supports, rather than on the increase of the supported area or the change in the stiffness of the barge.

Furthermore, concerning the behavior of the caisson, when interacting with the grillage and the vessel, it can be concluded that the stresses are uniformly distributed across the length of the skirts of the caisson, with very high peaks existing in the base of the caisson and at the points were the supports are placed (Figures 4.2 and 4.3). In addition, there are some peaks in stresses, which appear on top of the skirt in the position of the stiffeners of the lid. This is an indication of the load transferred from the top of the caisson and through the stiffeners to the rest of the skirt and finally to the supports and the barge. The high stresses in the location of the stiffeners, seem to be converged towards the supports and thus, creating much higher stresses in the base of the caisson, where the supports exist (Figure 4.4). Finally, for the examined load combination and for every case of boundary condition, the caisson is unlikely to develop any buckling behavior on the skirt.

The final research question has been replied by performing the parametric study. Analytically, even though the values of the stresses in the supported area change, the trend distribution of every stress component remains the same. The equivalent stresses in the base perimeter, show very high spikes at the edges of the supports, indicating that the forces are distributing from the top of the caisson to the barge through the edges of the supports (Figure 4.18). The analysis was expanded at a point, where is realized that the most important component is the bending stress in tangential(Θ) direction and hence is the one that should be reduced for the most optimal support condition. Tables 4.4 and 4.5, prove that the largest reduction takes place when the unsupported area, between the supported segments is reduced. In terms of deformation the results demonstrate that in vertical direction(z), the more the length of the support increases, the less the vertical deflection of the barge (Figure 4.15). With regard to radial(r) and tangential(Θ) direction, the deflection exists only in the unsupported area and its value is reduced once again, only when the unsupported area between the supported segments is also reduced (Figures 4.17 and 4.16).

After all of the analysis, is concluded that the most influence in the large deformations and the peaks in stresses in the caisson's perimeter has the length of the unsupported area between two supports. As aforementioned, the focus in the design of the grillage should not be given at increasing the length of the supported segments, but should be in reducing the unsupported area and managing to find the most optimal distance between the supports, in order for the caisson to experience the lowest deformations and the lowest stresses. The comparison of the parametric cases result in the most optimal configuration of transporting the caisson, which is case D. Case D is also examined in the non-linear analysis, from which is found that the peaks in stresses are acceptable and thereby strengthen the results of the linear analysis and the opinion that is the appropriate support case, out of those reviewed. It is important to mention that when the focus of the design is to reduce the unsupported area and not to increase the length of the support there could be an economical benefit as well. By taking into account once more the examined cases, it seems that case D has the same number of supported segments and therefore the same economic value in terms of materials used, as case B. However, the results in case D are much more beneficial than case B. Thus, it is also possible to conclude that the most optimal grillage design does not necessarily mean the most costly as well.

5.2. Recommendations

Although this study sets up the ground for some important aspects of the transportation of the suction jacket caisson and the influence of the boundary conditions that they have on its behavior there are some limitations that should be considered. First and foremost, the first limitation has been set during the design of the caisson. In the beginning of the analysis, the caisson was designed by selecting typical dimensions of this structure. The results and the complexity of the project has a great influence from the slenderness of the structure (D/t ratio) and by using the typical dimensions of the caisson, this is expected to cover similar, most often used dimensions and produce similar results. However, when the dimensions are extremely altered (i.e. D=11mm and t=70mm) this may lead to different results as well.

Furthermore, the loading conditions applied can be considered as another limitation. More specifically, during the transportation of the caisson, there are different types of loading combinations acting on the structure during the transportation. The combination applied in this case might be the most dominant one according to the actual project, however there might be another condition based on a loading analysis, which might cause larger stresses or buckling failure. Besides the loading conditions, the boundary conditions are an important factor considered in this project. The supports are applied by taking into account a specific loadout and seafastening procedure and a specific orientation of the supports, which allows for the total receipt of loads from the supports, since they are placed in the same direction. If the location of the supports changes and their orientation is shifted by 45degrees, the supports now exist on the outside direction of the coordinate system and therefore the behavior of the caisson might be altered and the supports might be less effective to withstand the applied loads.

Out of all the prior-mentioned constraints, even though every one of them has a great impact on the results, it is conceivable that the most influential one is the loading condition. According to the definition

of stresses and the factors, which affect buckling, a different load combination may result in different outcomes of the analysis and thus, lead to insufficient structural capacity and failure of the system, either in buckling and/or yielding. Therefore, regarding the limitations of the analysis it is recommended that this topic may be further investigated as follows:

- Examining the caisson by considering radically different and exaggerated dimensions for diameter and thickness of the caisson, so that to change excessively the slenderness of the structure.

- Perform a loading sensitivity analysis, which will result in alternative load combinations and examine the behavior of the caisson under these differing conditions. During the transportation the structure experiences various of loading combinations, which may cause compressive failure or buckling.

- Examining the caisson under alternative options in boundary conditions than the ones examined in this case study. This might provide a better solution in the grillage design and/or find a more optimal configuration for the support of the structure.

- Since the structure experiences in reality cycling loading during transportation, it is useful to examine the system for fatigue failure as well.

- An economic study might be also insightful about the expenses that may be incurred by the aforementioned cases of support. This will provide a further explanation about the optimization of the grillage design when it comes to reducing the unsupported area between two supports.

Bibliography

[1] EN-1993-1-1. *Design of steel structures - Part 1-1: General rules and rules for buildings*. NEN, 2006.

[2] EN-1993-1-5. *Design of steel structures - Part 1-5: Plated structural elements*. NEN, 2007.

[3] EN-1993-1-6. *Design of steel structures-part 1-6:General-Strength and Stability of Shell Structures*. NEN, 2006.

[4] J. E. Akin. *Finite Element Analysis Concepts: Via SolidWorks*. World Scientific, 2010, pp. 182–188.

[5] S. Bhattacharya. *Wind Energy Engineering*. University of Surrey, Guildford, 2017, pp. 221–242.

[6] DNVGL-OS-C102. *Structural design of offshore ship-shapped units*. DNVGL, 2020.

[7] DNVGL-RP-C208. *Determination of structural capacity by non-linear finite elements analysis methods*. DNVGL, 2019.

[8] DNVGL-ST-N001. *Marine operations and marine warranty*. DNVGL, 2018.

[9] B. Y. E. Ellobody R. Feng. *Finite Element Analysis and Design of Metal Structures*. Butterworth Heinemann, 2014, pp. 56–71.

[10] G. Houlsby et al. “Field trials of suction caissons in clay for offshore wind turbine foundations”. In: *Géotechnique* 55 (2005), pp. 287–296.

[11] NEN-EN-10025. *Hot rolled products of structural steels*. NEN, 2004.

[12] N. Ray et al. “Hex-dominant meshing: Mind the gap!” In: *Computer-Aided Design* 102 (2018), pp. 94–103.

[13] M. Tsota. “Transportation of Suction caisson jackets”. In: *Master Literature Thesis, TU Delft* (2022).

[14] www.ansys.com. *The Fundamentals of FEA Meshing for Structural Analysis*. 2021. URL: `https://www.ansys.com/blog/fundamentals-of-fea-meshing-for-structural-analysis`.

A
Calculations

Calculations of the stiffener's dimensions on the lid

Assuming that the vertical realistic force acting on top of the caisson is of value: $F := 30000\ kN$
$beam\_depth := 2000\ mm$ and $tlid := 45\ mm$ (Based on realistic project)
Since six(6) stiffeners are placed on top of the lid, an amount of the force is taken by each of them. For the calculations, it is assumed that 40% of the total force is taken by one of the stiffeners, which amounts to $Fz := 12000\ kN = 1,2 \cdot 10^{7}\ N$.

The stiffeners combined with the lid, appears as a I beam:
Since S355 was selected for the construction, the yield limit amounts to: $fy := (355) = 355\ \frac{N}{m^2}$

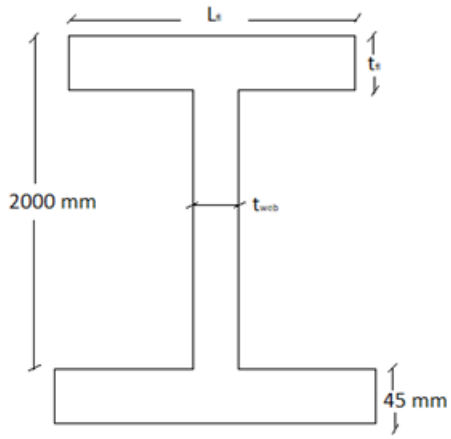

Surface area of the web:

$$Aweb := \frac{Fz}{\left(\frac{fy}{\sqrt{3}}\right)} = 58548\ kg\ mm^2$$

$$tw := \frac{Aweb}{2000\ mm} = 29,2741\ kg\ mm$$

For including the value of 29mm and safety reasons, the thickness of the web is considered $tweb := 35\ mm$

For flange is considered that F is taken by the 3 frames, resulting in 10000 kN per frame. Moment acting on 1 frame:

$$M := \frac{\left(\frac{F}{3}\right) \cdot l}{4}$$ where l is caissons diameter: $l := 10\ m$

Thus: $M = 2,5 \cdot 10^{7}\ J$

Force acting on flange: $\frac{M}{beam\_depth} \cdot \frac{3}{5} = 7,5 \cdot 10^{6}\ N$

Dividing with allowable yield stress limit: $Aflange := \frac{7500000}{355} = 21127\ mm^2$

Considering thickness of the flange as $tfl := 50\ mm$

$$Lfl := \frac{Aflange}{tfl} = 4,2254 \cdot 10^{5}\ m$$

Therefore, for safety reasons the length of the flange is considered as $Lf := 550\ mm$

Figure A.1: Calculation of dimensions of a stiffener on top of the lid

Moment of inertia for the I deck beam (Calculated from plate girder excel sheet):

$Iy := 8,52 \cdot 10^{10}\ mm^4 = 0,0852\ m^4$

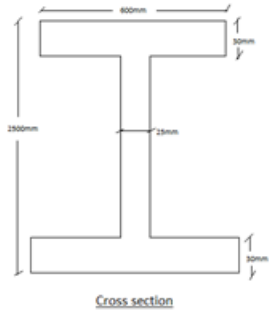

Cross section

Total applied vertical load (Calculated in excel):

$Fz := 2,73 \cdot 10^{7}\ N$

Taking into account that we are using 4 supports, we make the assumption that the load is equally devided in the 4 supports:

$F\_support := \frac{Fz}{4} = 6,825 \cdot 10^{6}\ N$

The load is applied in the middle of each support and is equally distributed to the sides of the seafastening connections in order to be tranfered afterwards to the grillage frame. Thus, we can assume for example that in support C the load in each side of the suuport is:

$Fc := \frac{F\_support}{2} = 3,4125 \cdot 10^{6}\ N$

The length between two bulkheads is an assumption, matching though to real dimensions of a barge grillage.

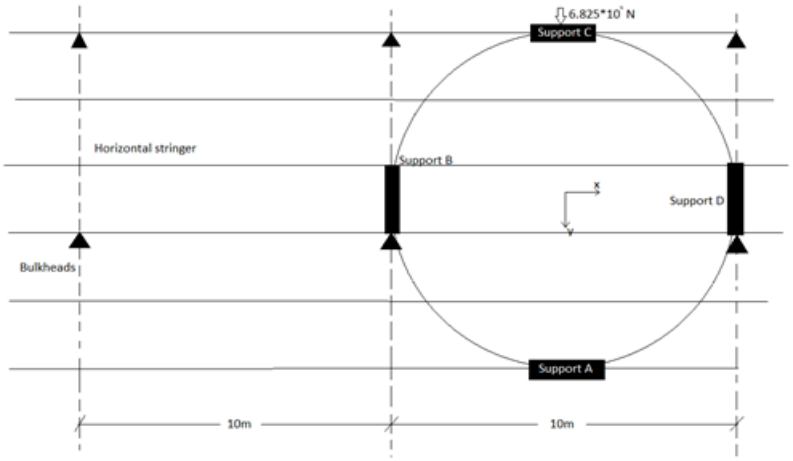

Considering the horizontal stringer with the bulckheads as horizontal simple supported beam, it is possible to calculate the deformation in support B, which will be simulated as the deformation of the beam with a force applied in the middle:

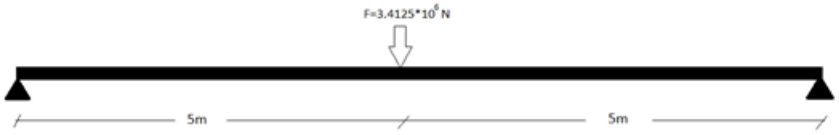

$E := 210\ GPa$

$l := 10\ m$

$\delta := \frac{Fc \cdot l^{3}}{48 \cdot E \cdot Iy} = 3,9735\ mm$

From the calculated deformation in support C we can estimate the stiffness that will be added in the support:

$k := \frac{Fc}{\delta} = 8,5882 \cdot 10^{5}\ \frac{N}{mm}$

Because the values in Ansys is in N/mm^3, we should devide the stiffness with the area of the segment that is going to be applied.

$A := 34720\ mm^2$

$kz := \frac{k}{A} = 24,7355\ \frac{N}{mm^3}$

The result was also confirmed in Ansys by inserting the values of $kz = 24,7355\ \frac{N}{mm^3}$ and the results showed a deformation of 3.37mm in support C.

For the horizontal stiffnesses ky and kx the values were increased by $85882 \cdot 10^{6}$ N/mm. In ansys for simplisity the value was rounded up to $9 \cdot 10^{6}$ N/mm.

Figure A.2: Calculation of stiffness of a barge